



Geochemistry, Geophysics, Geosystems

RESEARCH ARTICLE

10.1029/2019GC008749

Key Points:

- An Oligocene exhumation event, associated to the last phases of the West Antarctic Rift System, is widespread along both the margins of the Ross Sea
- The Central High has been identified as a major ice flow divide in the Ross Sea
- The West and East Antarctic Ice Sheets moved according to the balanced ice flow model during the Last Glacial Maximum

Correspondence to:

M. Zattin,
massimiliano.zattin@unipd.it

Citation:

Li, X., Zattin, M., & Olivetti, V. (2020). Apatite fission track signatures of the Ross Sea ice flows during the Last Glacial Maximum. *Geochemistry, Geophysics, Geosystems*, 21, e2019GC008749. <https://doi.org/10.1029/2019GC008749>

Received 8 OCT 2019

Accepted 11 SEP 2020

Accepted article online 22 SEP 2020

Apatite Fission Track Signatures of the Ross Sea Ice Flows During the Last Glacial Maximum

X. Li¹ M. Zattin¹ and V. Olivetti¹

¹Department of Geosciences, University of Padova, Padova, Italy

Abstract The catchment for the Ross Sea ice includes both the East and the West Antarctic ice sheets, but the mass balance is a direct response to climate change. Our work is aimed to reconstruct the ice flows after the Last Glacial Maximum and is based on apatite fission track data from samples collected from 18 piston cores across the Ross Sea embayment. Fission track ages have been divided into meaningful populations and then compared with bedrock ages from West and East Antarctica. Furthermore, fission track lengths have been measured on each population and then compared through forward modeling with thermal histories derived from literature. The widespread presence of apatites with cooling ages of about 30–40 Ma reveals a main exhumation phase of the Transantarctic Mountains during the Oligocene associated to the last phases of the West Antarctic Rift System. Furthermore, the presence of key marker apatites (e.g., younger than 21 Ma or older than 230 Ma) allows to identify the Central High as a major ice flow divide.

1. Introduction

The Ross Sea embayment is a crucial area for understanding the ice dynamics as a direct response to climate changes. The Ross Sea embayment, being enclosed for two thirds by the two Antarctic Ice Sheets, is the natural storage of the sediments that are produced by subglacial and aerial erosion and transported by glacial flows. The glaciogenic sediments deposited in the Ross Embayment record the evolution of both the East and West Antarctic Ice Sheets, whose dynamics and stability is still debated, although a number of sediments provenance (see Licht & Hemming, 2017, for a recent review), numerical modeling (e.g., Dolan et al., 2018; Golledge et al., 2012; Pollard & Deconto, 2009), and geomorphological studies have been carried out (Licht & Andrews, 2002; Mosola & Anderson, 2006).

Overall, the ice flow evolution during the Last Glacial Maximum (LGM) in the Ross Sea has been interpreted according to three different models (Figure 1): (1) West Antarctic Ice Sheet (WAIS)-dominated model, based mainly on provenance studies, that predicts a flow from WAIS to a relatively narrow drainage along the western Ross Sea coastline (Figure 1b) (Stuiver et al., 1981); (2) WAIS-East Antarctic Ice Sheet (EAIS) balanced model, in which the confluence of West Antarctic ice and East Antarctic ice occurs in the central Ross Sea and ice contribution from East Antarctica and West Antarctica is equivalent (Figure 1c) (Denton & Hughes, 2000; Licht et al., 2005; Licht & Fastook, 1998); and (3) EAIS-dominated model based on numerical modeling, in which the WAIS strongly influences the eastern Ross Sea and the EAIS contributes with most of the ice to the central and the western Ross Sea (Figure 1d) (Golledge et al., 2012).

The definition of ice flow pathways during the LGM is highly complicated by repeated ice advance and retreat, the huge sea area, and low sample density, despite several hundred sediment cores have been collected. A major advance in understanding the glacial history came with the development of multibeam swath bathymetry (e.g., Bart & Cone, 2012; Mosola & Anderson, 2006; Shipp et al., 1999, 2002), assuming that the present-day geomorphic features formed during the most recent glacial advance and that during the peak LGM thick ice from the WAIS was grounded in the western Ross Sea. Diachronicity of expansion and retreat of the ice sheets through the Ross embayment such as the very different physiographic settings and the lack of reliable radiocarbon ages preclude from unambiguous reconstructions. However, understanding of ice sheet history has increased significantly over the past decade because of an increasing number of provenance studies of glaciogenic sediments based on different approaches such as mineral composition of the sandy fraction (e.g., Anderson et al., 1992; Balshaw, 1980; Denton & Hughes, 2000; Farmer et al., 2003, 2006; Hauptvogel & Passchier, 2012; Hughes, 1977; Licht et al., 2005; Licht &

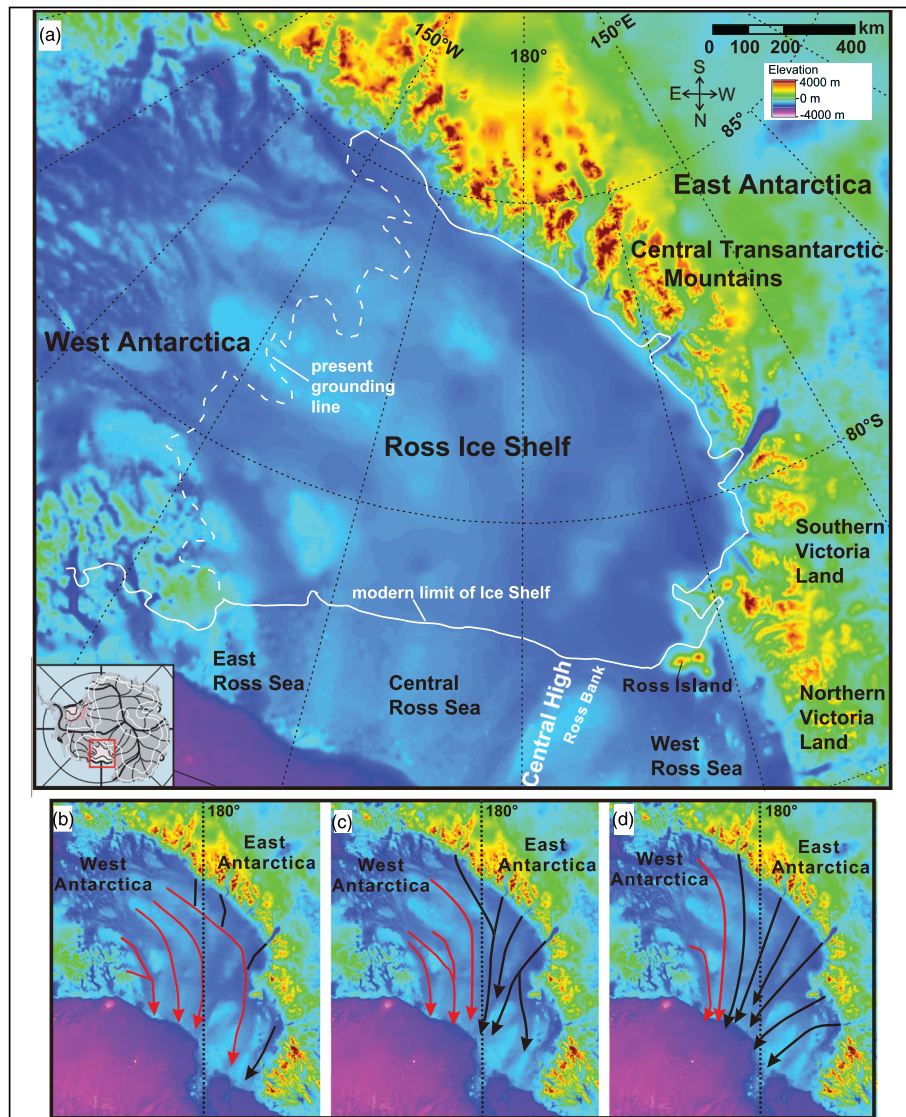


Figure 1. (a) Location of the study area. (b–d) Three different interpretations of the flow lines during the LGM. Panels (b) and (c) are based on provenance studies, whereas panel (d) is based on numerical modeling (according to Denton & Hughes, 2000; Golledge et al., 2012; Licht et al., 2005; Licht & Fastook, 1998; Stuiver et al., 1981). ERS: East Ross Sea; CRS: Central Ross Sea; WRS: Western Ross Sea.

Fastook, 1998) or geochronological & thermochronological studies (e.g., Farmer & Licht, 2016; Li et al., 2019; Licht et al., 2014; Licht & Hemming, 2017; Olivetti et al., 2013, 2015; Perotti et al., 2017; Zattin et al., 2010, 2014). The key for interpreting the provenance data is based on the comparison of the petrographic composition of the sediment with the mineralogy of potential source areas. In the specific case of detrital thermochronology, we can compare the age distribution in the sediments with the cooling ages in the bedrock. This approach is well working with glaciogenic sediments as they provide a valuable amount of key data concerning the history of sources that were eroded by the ice and thus a record of ice sheet history. Moreover, the limited exposure of bedrock geology and the inaccessibility of remote areas in Antarctica make detrital thermochronology a preferential tool to explore the complexity of the evolution of the Transantarctic Mountains (TAM) and also of West Antarctica. This paper is based on detrital apatite fission track data obtained on samples of post-LGM age from 18 piston cores across the Ross Sea. The distribution of different age populations reveals the Central High as a major ice flow divide in the Ross Sea and a widespread phase of exhumation all around the Ross Sea embayment.

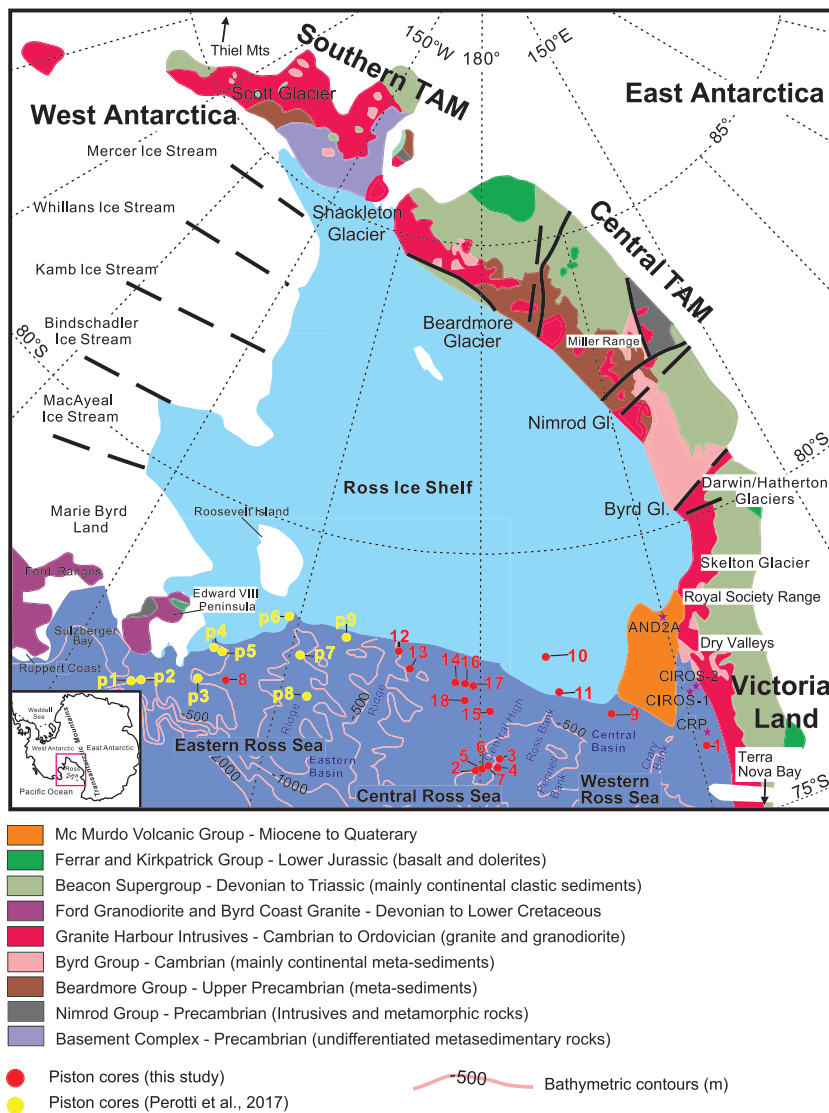


Figure 2. Geological map of the Ross Sea, West Antarctica, and East Antarctica with the distribution of piston cores (red dots for samples in this paper and yellow dots for samples) published by Perotti et al. (2017). Bedrock map is according to Bushnell and Craddock (1970) and Licht et al. (2005). Bathymetric features are according to Mosola and Anderson (2006).

2. Geological Setting

2.1. The Ross Embayment

The Ross Embayment is bounded by the TAM to the east and by the Marie Byrd Land to the west (Figure 2). It comprises the Ross Sea and the Ross Ice Shelf, the largest ice shelf worldwide, nourished by glaciers stream draining about $1.65 \times 10^6 \text{ km}^2$ from the EAIS and $0.75 \times 10^6 \text{ km}^2$ from the WAIS (Rignot et al., 2008). The bathymetric features of the Ross Sea consist of six northeast trending troughs separated by the so-called Mawson, Crary, Pennell, and Ross banks in the western Ross Sea and less prominent ridges in the east (Figure 2). The continental shelf has gentle gradients, with a depth seaward of about 500 m and a shelf break at 500–600 m (Mosola & Anderson, 2006; Tinto et al., 2019).

The LGM ice extent in the Ross Sea has been identified at the shelf break in the central and eastern Ross Sea and slightly seaward of Coulman Island in the western Ross Sea (Anderson et al., 1992; Domack et al., 1999; Kellogg et al., 1979; Licht et al., 1996, 1999; Licht & Andrews, 2002; Shipp et al., 1999). LGM till thickness is

variable, but all data point to eastern and central Ross Sea tills thicker than western Ross Sea tills (Licht et al., 2005; Shipp et al., 1999).

The typical stratigraphic succession of the deposits sampled in piston cores from the western Ross Sea consists of an upward progression from till to proximal glacial marine to distal glacial marine sediments that generally show increasing abundance of diatomaceous material upwards (Anderson et al., 1992; Domack et al., 1999; Licht et al., 1999; McKay et al., 2008). This succession records the progressive landward shift in the retreating grounding line across the continental shelf and the eventual onset of periodic open-marine conditions in the western Ross Sea (Anderson et al., 2014). Cores from the eastern Ross Sea generally consist of predominantly terrigenous glacial marine sediments resting in sharp contact on till. The absence of an upper diatomaceous facies in the central and eastern Ross Sea indicates the presence of widespread and persistent sea ice cover that has restricted primary productivity (Dunbar et al., 1985; Licht & Andrews, 2002; Mosola & Anderson, 2006).

2.2. The Geology of West Antarctica

Marie Byrd Land is one of the major crustal blocks forming the West Antarctica. Its western portion is situated today adjacent to the Ross Sea (Figure 2) (Spiegel et al., 2016), and it is largely covered by the WAIS and mostly grounded below sea level (Licht et al., 2005) although there the best exposed rock outcrops in West Antarctica can be found (Perotti et al., 2017).

The oldest rock is given by the Neoproterozoic-Cambrian Swanson Formation, made of low grade metasediments, which was intruded by the Devonian-Carboniferous Ford Granodiorite suite (Adams, 1986; Bradshaw et al., 1983; Pankhurst et al., 1998; Weaver et al., 1991). The Swanson formation crops out mainly in the Ford Ranges in western Marie Byrd Land (Figure 2) (Brand, 1979). The Swanson Formation and the Ford Granodiorite suite are both intruded by the Byrd Coast Granite (Korhonen et al., 2010a, 2010b; Weaver et al., 1992). The igneous activity involved the regions of Ruppert and Hobbs Coast (110–101 Ma) (Mukasa & Dalziel, 2000) and Ford Ranges-Edward VII Peninsula (Figure 2) (Pankhurst et al., 1998; Weaver et al., 1992). Crustal extension during the Cretaceous produced also the emplacement of mafic dykes throughout the Ford Ranges (Saito et al., 2013; Siddoway et al., 2005). Locally Swanson Formation and intrusives rocks are affected by high-grade metamorphism during Devonian-Carboniferous and Cretaceous forming the today exposed migmatitic dome of the Fosdik Mountain (Siddoway, Baldwin, et al., 2004; Siddoway, Richard, et al., 2004). The Cretaceous phase of deformation was followed by a rapid exhumation testified by low-temperature thermochronological data coming from Edward VII Peninsula and Ford Range, showing in general a cluster of mid-Cretaceous ages for apatite and zircon fission track dating (Adams et al., 1995; Lisker & Olesch, 1998; Zundel et al., 2019). During the Cenozoic, starting from about 35 Ma, the region of Marie Byrd Land was affected by an intense alkaline volcanism and uplift (LeMasurier et al., 2011).

2.3. The Geology of East Antarctica

The portion of East Antarctica surrounding the Ross Embayment is formed by the TAM. The basement units of the TAM representing the exhumed roots of the late Neoproterozoic to early Paleozoic Ross Orogen (Cook & Craw, 2002; Findlay & Meyer, 1984; Gunn & Warren, 1962), were intruded by the Cambrian-Ordovician Granite Harbor Intrusive Complex (Allibone et al., 1993; Gunn & Warren, 1962). Uplift and erosion followed pluton emplacement, furthermore resulting in the regionally extensive Kukri surface that provide a first-order element in the geological history of the TAM. The Kukri surface is recognizable throughout the TAM, testifying the end of the orogenic phase and the onset of continental sedimentation that evolved diachronously along the TAM. Above the Kukri Peneplain, the mainly continental Devonian to Triassic Beacon Supergroup was deposited (Barrett, 1991). During the Jurassic, a large magmatic event, both intrusive and effusive, took place along the TAM for more than 3,500 km (Ferrar Large Igneous Province; Elliot & Fleming, 2008). An approximately 160 Ma gap separates the Jurassic magmatism from the late Cenozoic alkaline volcanism of the McMurdo Volcanic Group. The emplacement of the Ross Island volcanoes resulted in significant modification of the McMurdo Sound paleogeography (Kyle, 1981, 1990).

The present-day exposure of the TAM is the result of different exhumation episodes, well recorded by thermochronology techniques. The former interpretation consisting in a stepwise monotonous exhumation since Jurassic for the whole TAM is currently under revision and many authors provided evidence for (i)

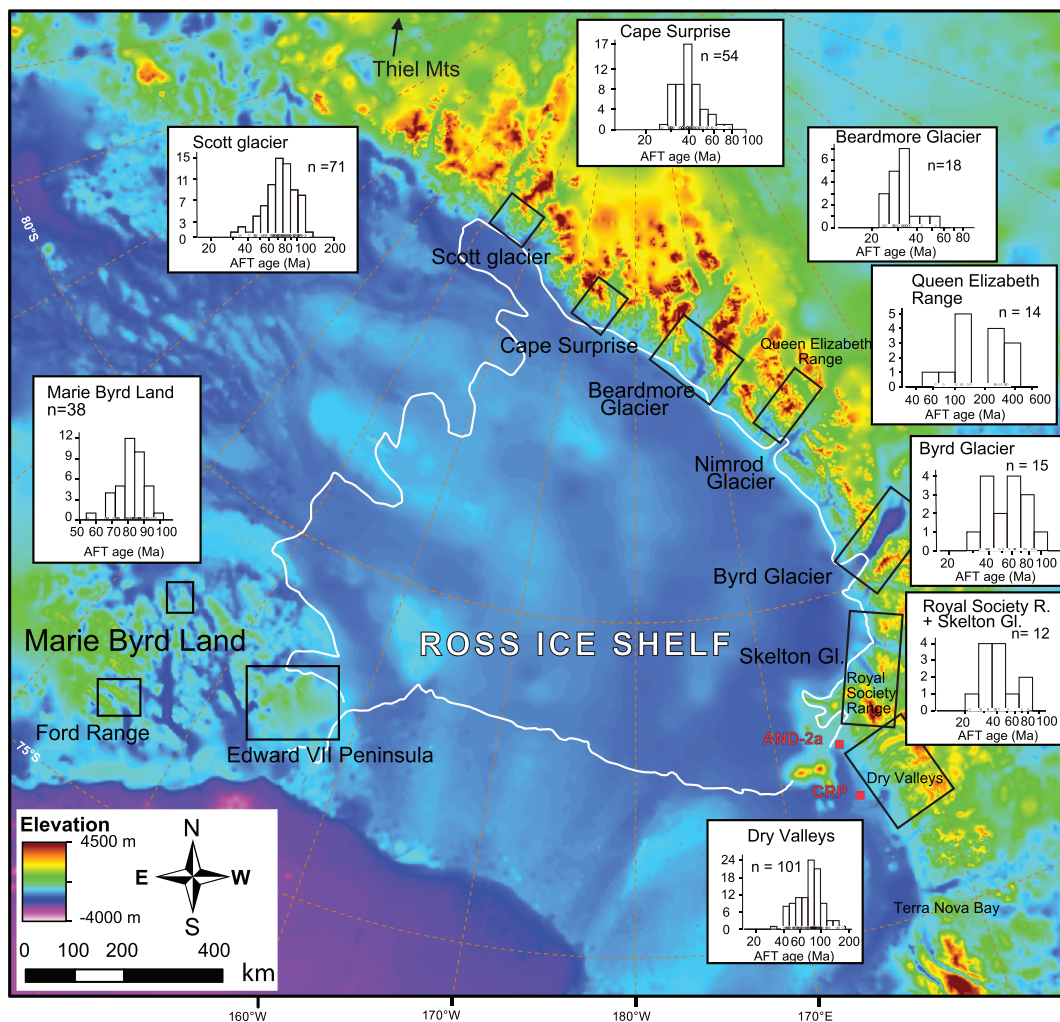


Figure 3. Compilation of AFT data around the Ross Sea Embayment (see text for references).

Jurassic-Cretaceous burial and post-Eocene exhumation (Lisker & Laufer, 2013; Prenzel et al., 2013, 2014, 2018) and (ii) an along-strike regional variability in the amount of exhumation (Olivetti et al., 2018).

One of the oldest events, based on fission track ages, has been proposed in the Thiel Mountains (out of map, Figures 2 and 3) and is dated at 165–150 Ma (Fitzgerald & Baldwin, 2007). Middle Cretaceous apatite fission track (AFT) ages (approximately 125–90 Ma) are reported in the Scott Glacier region (Fitzgerald & Stump, 1997), the central TAM (Fitzgerald, 1994), & both south and northern Victoria Land (Balestrieri et al., 1997; Fitzgerald, 1992; Fitzgerald & Gleadow, 1988; Lisker, 2002; Lisker et al., 2006; Storti et al., 2008; Welke et al., 2016). However, the lack of extensive thermal modeling prevents a clear definition of timing and extent of an overall exhumation during the Cretaceous. The Rb-Sr and $^{40}\text{Ar}/^{39}\text{Ar}$ age determinations on apophyllite in Ferrar basaltic rocks (Molzahn et al., 1999), Rb-Sr relationships, K-Ar dates, and palaeomagnetic pole positions in north Victoria Land (Faure & Mensing, 1993; Fleming et al., 1993) seem to support the Cretaceous exhumation in many sectors of the TAM (Elliot et al., 2015).

Based once again on fission track data, major Cenozoic exhumation and uplift of the TAM were initiated during the Eocene-Oligocene between 55 and 45 Ma or between 40 and 30 Ma depending on regional variability and authors (Fitzgerald, 2002; Prenzel et al., 2018). Oligocene apatite fission track ages are regionally clustered and patchy distributed all along the TAM, showing that some portions of the TAM eroded at this time. This event is well described by thermochronology ages on bedrock (e.g., Fitzgerald, 1994; Miller et al., 2010; Olivetti et al., 2018; Zattin et al., 2014) and on detrital grains (Li et al., 2019;

Olivetti et al., 2015; Zattin et al., 2010, 2012). An erosion event younger than Oligocene is recorded by very few thermochronological ages, but it is supported by thermal modeling and geomorphic evidence (Fitzgerald, 2002; Paxman et al., 2019; Prenzel et al., 2018).

2.4. Overview of Ice Flow Dynamics of the Ross Sea

2.4.1. Eastern Ross Sea

A review of the existing literature (Anderson et al., 1992; Balshaw, 1980; Farmer et al., 2006; Hughes, 1977; Licht et al., 2005; Perotti et al., 2017) indicates that the eastern Ross Sea (ERS in Figure 2) tills are provided uniquely by the WAIS. This is proved, for example, by clay mineralogy of tills, which shows the highest concentration of smectite in the ERS troughs, whereas the content in the western Ross Sea (WRS) and the central Ross Sea (CRS) (Figure 2) troughs is lower (Balshaw, 1980). Combining the view from Hughes (1977) that the WAIS expanded following the Ross Sea bathymetry, Balshaw (1980) speculated that high concentration of smectite in the ERS is probably sourced from Bindschadler, MacAyeal, and Echelmeyer Ice Streams in West Antarctica. Further evidence derives from petrographic composition (pebble, coarse sand, and heavy minerals). Different works (e.g., Anderson et al., 1992; Licht et al., 2005; Perotti et al., 2017) show a significant variability from east to west across the Ross Sea. The ERS sand fraction is composed of schist and smaller quantities of gneiss, rounded quartz, and granite, which is quite different from the WRS tills sand fraction dominantly composed of rounded quartz, granite, diamicton fragments, volcanic glass, and minor diabase and litharenite (Anderson et al., 1992). Furthermore, ERS tills are compositionally similar to West Antarctica tills, particularly in their abundance of quartz and dearth of mafic and extrusive lithic components (Licht et al., 2005). Besides, the isotopic compositional data also show strong similarities between West Antarctica and ERS (Farmer et al., 2003; Licht et al., 2005). U-Pb zircon age populations (100–110, 450–475, and 330–370 Ma) found in tills located in Bindschadler and Kamb ice streams are consistent with ERS tills (Licht et al., 2014). Multianalytical provenance analysis (petrographic analysis of gravel-sized clasts, geochronology, and thermochronology) of samples in the ERS and Sulzberger Bay by Perotti et al. (2017) also implied a WAIS source. As a general pattern, the common view is that the ERS is dominated by ice derived from West Antarctica, with minor if not null sources from East Antarctica.

2.4.2. Central Ross Sea

The analysis of sediment sources in the CRS is much more complex. The works by Farmer et al. (2006) and Farmer and Licht (2016), based on Nd, Sr, and Pb isotopic signatures, indicate first that fine-grained detritus is the product of further comminution of coarser sediments. Comparison of present-day till isotopic data with existing data from fine-grained LGM tills in the CRS suggests that these were transported from East Antarctic ice that expanded through the TAM and indicates that the LGM sediments are a mixture of detritus eroded along the entire path of ice. However, the U-Pb zircon age distribution found in Whillans Ice Stream till (which is considered part of WAIS but partially originated in East Antarctica) is more similar to tills from the WRS and the CRS (Licht et al., 2014). The region of converging East and West Antarctic ice has been hypothesized to be the CRS (Denton & Hughes, 2000; Licht & Fastook, 1998). In fact, the diagrams representing the petrographic composition of CRS till samples show a mixture of East and West Antarctic sources (Licht et al., 2005). Furthermore, most CRS till samples contain mafic intrusive lithic and mafic mineral components, which have been observed almost exclusively in the WRS and East Antarctica till samples. On the contrary, the mafic component is essentially absent in the ERS samples (Licht et al., 2005). An East Antarctica source for CRS till is also indicated by the presence of an oolitic limestone fragment in one CRS sample (Licht et al., 2005). Oolitic limestone has been mapped only in rocks of the Holyoake Range near the Nimrod Glacier, which bisects the TAM (Bushnell & Craddock, 1970; Licht et al., 2005). Additionally, Nd and Sr analyses from CRS cores show low ε_{Nd} values, indicative of an East Antarctic source terrane (Farmer et al., 2003). Most if not all the analyses support therefore the idea that the confluence of the EAIS and WAIS during the LGM occurred in the CRS (Licht et al., 2005).

2.4.3. Western Ross Sea

Balshaw (1980) supposed that low smectite concentration in the WRS tills probably derived from Mercer, Whillans, and Kamb Ice Stream that flow from West Antarctica. Anderson et al. (1992) found that the WRS sand fraction is dominantly composed of rounded quartz, granite, diamicton fragments, volcanic glass, and minor diabase and litharenite, therefore pointing to a source from the Beacon Supergroup, Ferrar Group, McMurdo Volcanic Group, and exposures of biotite schists and gneisses near Priestly Glacier in East Antarctica. Licht et al. (2005) argued that the WRS till samples bear strong compositional similarity

Table 1
Information of Each Piston Core in This Work

Sample name	Cruise	Core	Latitude	Longitude	Water depth (m)	Core length (cm)
1	DF78	014-PC	-76.5	164	424	334
2	NBP94-07	070-PC	-76.405	-179.657	512	308
3	NBP94-07	093-PC	-76.76	178.535	298	359
4	NBP94-01	027-PC	-76.522	178.881	312	235
5	NBP94-07	078-PC	-76.493	-179.963	375	270
6	NBP94-07	079-PC	-76.487	179.949	295	151
7	NBP96-01	002-JPC	-76.452	179.881	373	419
8	NBP96-01	006-JPC	-77.222	-161.476	649	341
9	DF62-01	005-PC	-77.3333	170	805	76
10	DF78	012-PC	-78.267	175.25	538	271
11	DF76	001-PC	-77.45	174.8	695	544
12	DF76	003-PC	-78.2	-174.183	558	671
13	NBP00-01	001-PC	-78.019	-176.252	578	237
14	NBP94-07	039-PC	-77.924	-178	694	103
15	NBP95-01	017-PC	-77.452	179.05	732	202
16	NBP94-07	041-TC	-77.921	-178.26	716	32
17	NBP94-07	043-PC	-77.917	-178.822	725	241
18	NBP94-07	051-PC	-77.659	-177.789	678	125

to East Antarctic till samples and are distinctly different from West Antarctic till samples, supported by Nd and Sr isotopic analyses of the silt+clay fraction from the same samples analyzed by Farmer et al. (2003). Sand fraction of LGM glacier till indicates that WRS till samples exhibit mineralogic and lithological frameworks similar to East Antarctic till samples, whereas West Antarctica-derived ice streams did not advance into the WRS (Licht et al., 2005). The U-Pb zircon age distribution found in Whillans Ice Stream till is most similar to tills from the WRS and CRS (Licht et al., 2014). Studies of till provenance and the orientations of geomorphic features on the Ross Sea continental shelf show that ice with East Antarctic origins extended across the continental shelf west of 180° (Anderson et al., 2014). Provenance studies of offshore drillings (MSSTS, CIROS-2, CIROS-1, CRP-1, CRP-2/2A, CRP-3, AND-1B, and AND-2A) in McMurdo Sound in the WRS reflect local geological source terranes from TAM and outlet glaciers of East Antarctica draining ice into the WRS. Moreover, provenance studies of AND-1B and AND-2A (which record the last 20 Ma) by Zattin et al. (2010, 2012) show an ice pattern dominated by south to north trending flow lines parallel to the TAM in the WRS. In all, EAIS dominated the WRS, probably with an ice flow originated from the WAIS northward along the coast of TAM.

3. Material and Methods

This work is based on 32 samples from 18 piston cores obtained from the Antarctica Research Facility at Florida State University. They were drilled by different scientific cruises across the Ross Sea: DF78, NBP94-07, NBP94-01, NBP96-01, DF62-01, DF76, NBP00-01, NBP94-07, and NBP95-01 (Table 1). Subsamples for analysis were chosen from cores retrieved landward of the LGM grounding line in the Ross Sea. Actually, most of cores are distributed in the CRS (piston cores 2–7 and 12–17) near the longitude 180°. Other cores are located in the WRS (piston cores 1 and 9–11), whereas only piston core 8 is located in the ERS. Details on location are shown in Table 1. All the cores in this work yield samples of a stratigraphic age younger than the LGM. Each of the sample, collected in the sand levels, integrates about 5 cm of materials (depth shown in Table 2).

3.1. Apatite Fission Track Dating

All 32 samples have been dated by apatite fission track method, which allows to date the cooling of the rocks under ~110°C and to reconstruct their time-temperature path (Reiners & Brandon, 2006). Apatite grains have been separated from piston cores and then processed for fission track analysis through standard processing techniques. What could be dated for each sample are 20 to 198 grains could be dated for each sample. Single grain ages were calculated using the external-detector and the zeta-calibration methods (Hurford & Green, 1983) with International Union of Geological Sciences (IUGS) age standards (Durango and Fish

Table 2
Apatite Fission Track Data of Samples Collected From Piston Cores in the Ross Sea (the Location of Piston Cores Is Shown in Figure 2)

Sample name	Cruise	Depth (cm)	No. of crystal	P1 (%)	P2 (%)	P3 (%)	P4 (%)	P5 (%)	P6 (%)	P7 (%)
1	DF78-014	25–32, 102–107, 187–192, 242–247, and 297–302	189				98.8 ± 4.3 (23.2%)	139.7 ± 7.9 (30.8%)	204 ± 14.0 (28.9%)	293.2 ± 30.0 (13.7%)
2	NBP94-07-070	0–3	22	40.3 ± 3.6 (30.6%)	45.8 ± 3.1 (27.9%)	90.7 ± 4.9 (45.3%)	170.7 ± 15.1 (14.7%)	155.8 ± 7.4 (58.5%)	539.3 ± 103.4 (10.9%)	
3	NBP94-07-093	12–17 and 35–40	63	7.9 ± 1.7 (12.1%)	36 ± 2.8 (19.5%)	64.3 ± 4.7 (23.5%)	84.1 ± 4 (39.8%)	145.8 ± 6.9 (26.5%)	268.4 ± 13.7 (7.6%)	462.9 ± 36.7 (3.1%)
4	NBP94-01-027	12–17, 126–130, and 184–188	120	19 ± 1.9 (4.4%)	41.4 ± 2.35 (18.7%)	84.6 ± 6.1 (25%)	84.6 ± 8.1 (41.5%)	137.2 ± 8.1 (41.5%)	286.3 ± 25.9 (2.4%)	466.4 ± 35.7 (5.3%)
5	NBP94-07-078	77–82, 92–97, 132–137, 154–159, and 235–239	198	34 ± 2.6 (31.2%)	73.5 ± 3.7 (46.3%)	147.5 ± 7.5 (31.3%)	147.5 ± 7.5 (31.3%)	278.7 ± 19.3 (9.2%)		278.7 ± 19.3 (9.2%)
6	NBP94-07-079	5–10, 73–75, 95–100	57	30.9 ± 3.9 (13.2%)	55.2 ± 10.4 (26.6%)	64.4 ± 7.2 (33.3%)	64.4 ± 7.2 (51.1%)	149.6 ± 20.6 (15.6%)		
7	NBP96-01-002	1–3, 81–84, and 360–365	97				97.7 ± 10.4 (40.8%)	153.4 ± 24.6 (10.4%)		
8	NBP96-01-006	18–24	17				84.1 ± 7.9 (54.2%)	148.5 ± 18.4 (48.2%)		
9	DF62-01-005	28–32	40	20.8 ± 2.9 (33.3%)	28.3 ± 3.5 (43%)	61.2 ± 5.9 (48.8%)	88 ± 3.5 (31.6%)	149.6 ± 20.6 (15.6%)		
10	DF78-012	245–248	40				57.4 ± 6.55 (31.6%)	84.1 ± 7.9 (48.2%)		
11	DF76-001	280–287	36				63.6 ± 7 (41.6%)	132 ± 2.9 (54.7%)		
12	DF76-003	579–583	40				64 ± 7.1 (72.9%)	99.5 ± 23.4 (20.8%)		
13	NBP00-01-001	100–105	40	13.6 ± 6.8 (3.8%)					485.3 ± 253.4 (2.8%)	
14	NBP94-07-039	45–51	42	18.7 ± 6.3 (3.7%)					378.2 ± 108.4 (2.7%)	
15	NBP95-01-017	179–187	40	34.1 ± 4.6 (19%)	74.5 ± 6.5 (70.2%)					
16	NBP94-07-041	0–5	20	35 ± 8.5 (12.1%)						
17	NBP94-07-043	94–98	37				53.4 ± 9.7 (28%)			
18	NBP94-07-051	100–105	30				56.7 ± 8.8 (13.6%)	93.3 ± 10 (30.3%)	112.6 ± 4.6 (10.7%)	125.8 ± 8.5 (7.2%)
									144.3 ± 12.5 (56.1%)	

Note: Most samples have been obtained from merging subsamples collected at different depths in the same piston cores.

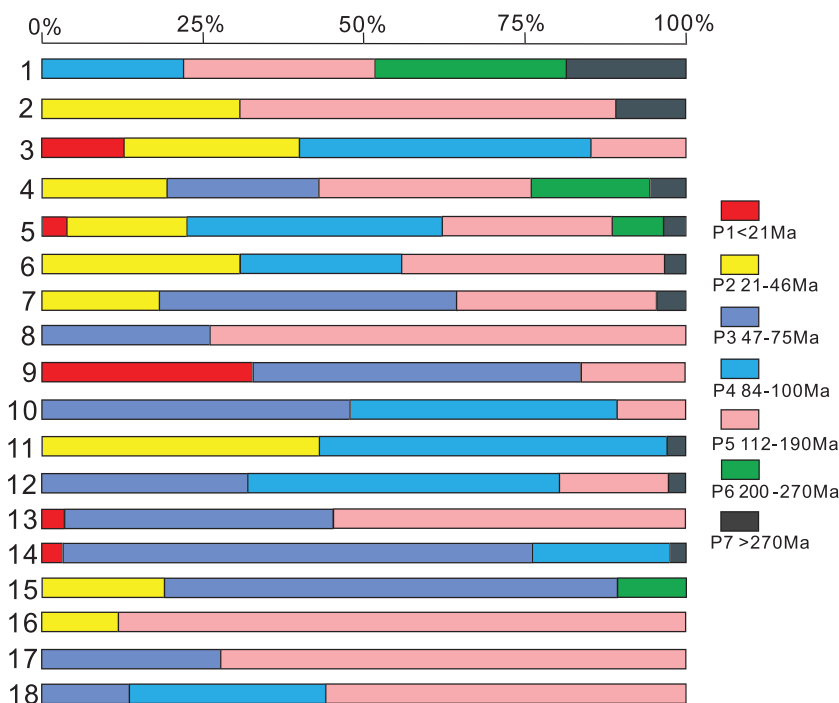


Figure 4. Distribution of apatite fission track age populations. The percentage scale on the top represents proportion of different populations (sample locations shown in Figure 2).

Canyonapatites) (Hurford, 1990) and a value of 0.5 for the $4\pi/2\pi$ geometry correction factor. The analyses were subjected to the χ^2 test (Gailbraith, 1981) to detect whether the data sets contained any extra-Poissonian age component. A χ^2 probability of less than 5% denotes a significant spread of single grain dates. After using standard analytical procedures, grain age distributions of each piston core were decomposed into different components (Table 2 and Figure 4) and plotted as combined radial and kernel density plots (Dietze et al., 2016) (Figure 5).

In order to check the kinetics of annealing of fission tracks for each sample, we also measured the Dpar (the arithmetic mean of fission track etch pit lengths measured parallel to the crystallographic *c* axis; Burtner et al., 1994; Donelick, 1993).

Track length measurement can provide a further information on the thermal history of the source rock. This procedure is routinely applied to bedrock samples as track length distribution from detrital grains could be strongly dependent from multiple source areas. Despite of this, in this work we measured fission tracks, but then, length data were then divided into different groups according to the age of the grain in which they were measured. Due to the quality of grains, as a whole, statistically meaningful length distributions have been measured on four populations from four piston cores (cores 1, 4, 5, and 7; Figure 6).

3.2. Multidimensional Scaling Method

The large single grain age data set here obtained has been analyzed by the multidimensional scaling method, which has been proved to be an easy and efficient statistical technique for comparison of complex detrital geochronological data (Vermeesch, 2013). Actually, it is a dimension-reducing exploratory data analysis tool but can capture the main features of detrital data sets. It is a robust and flexible superset of the principal component analysis, which makes fewer assumptions about the data and produces a “map” of points on which “similar” samples cluster closely together, and “dissimilar” samples plot far apart (Vermeesch, 2013). We use the multidimensional scaling user-friendly interface provided by the website (<http://mudisc.london-geochron.com>). In order to maximize the statistical significance of the data, we excluded some samples with few grains (samples 2, 8, and 16) (Figure 7).

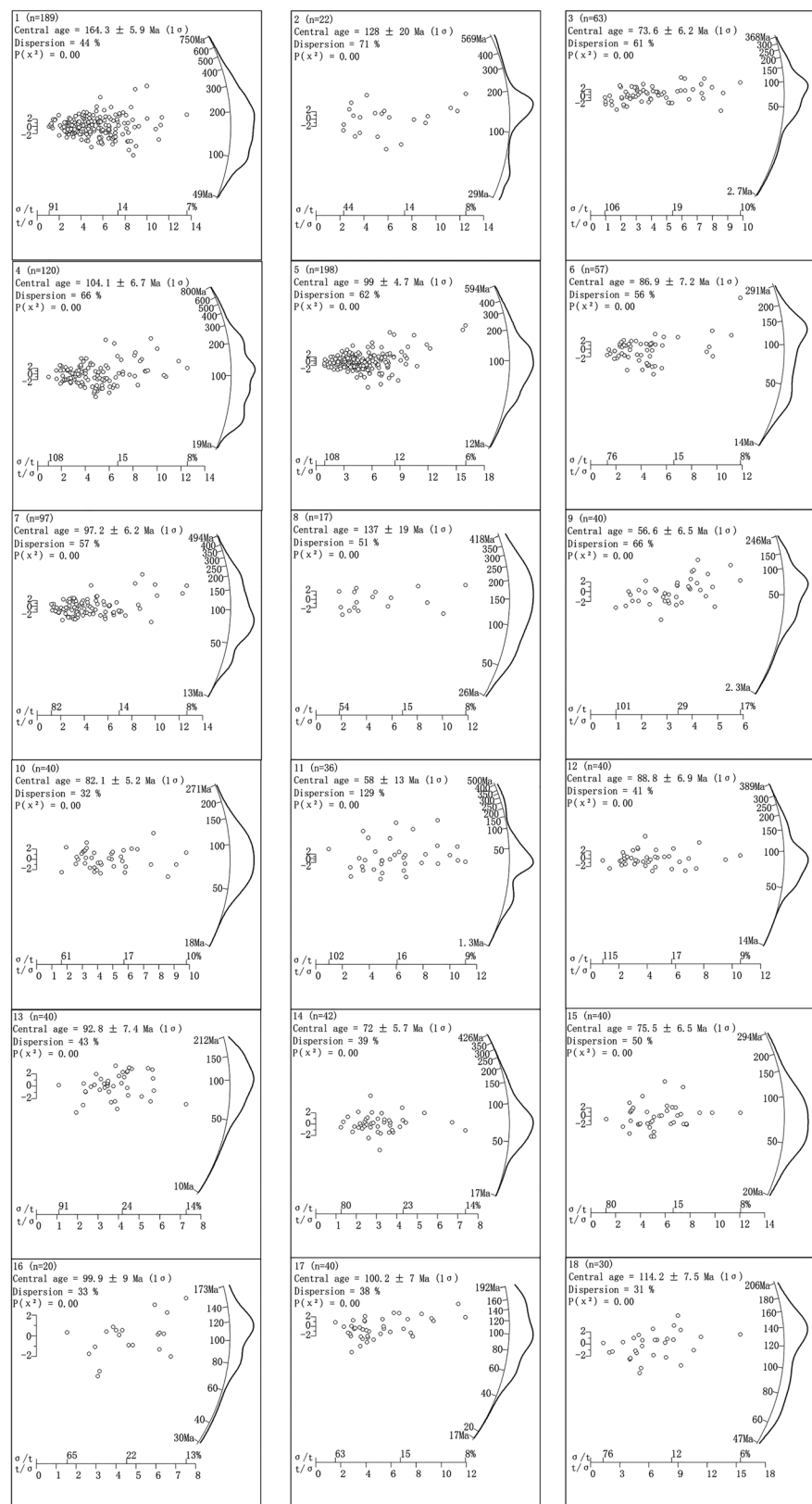


Figure 5. Abanico plots (Dietze et al., 2016) of apatite fission track age data in the Ross Sea (sample locations shown in Figure 2).

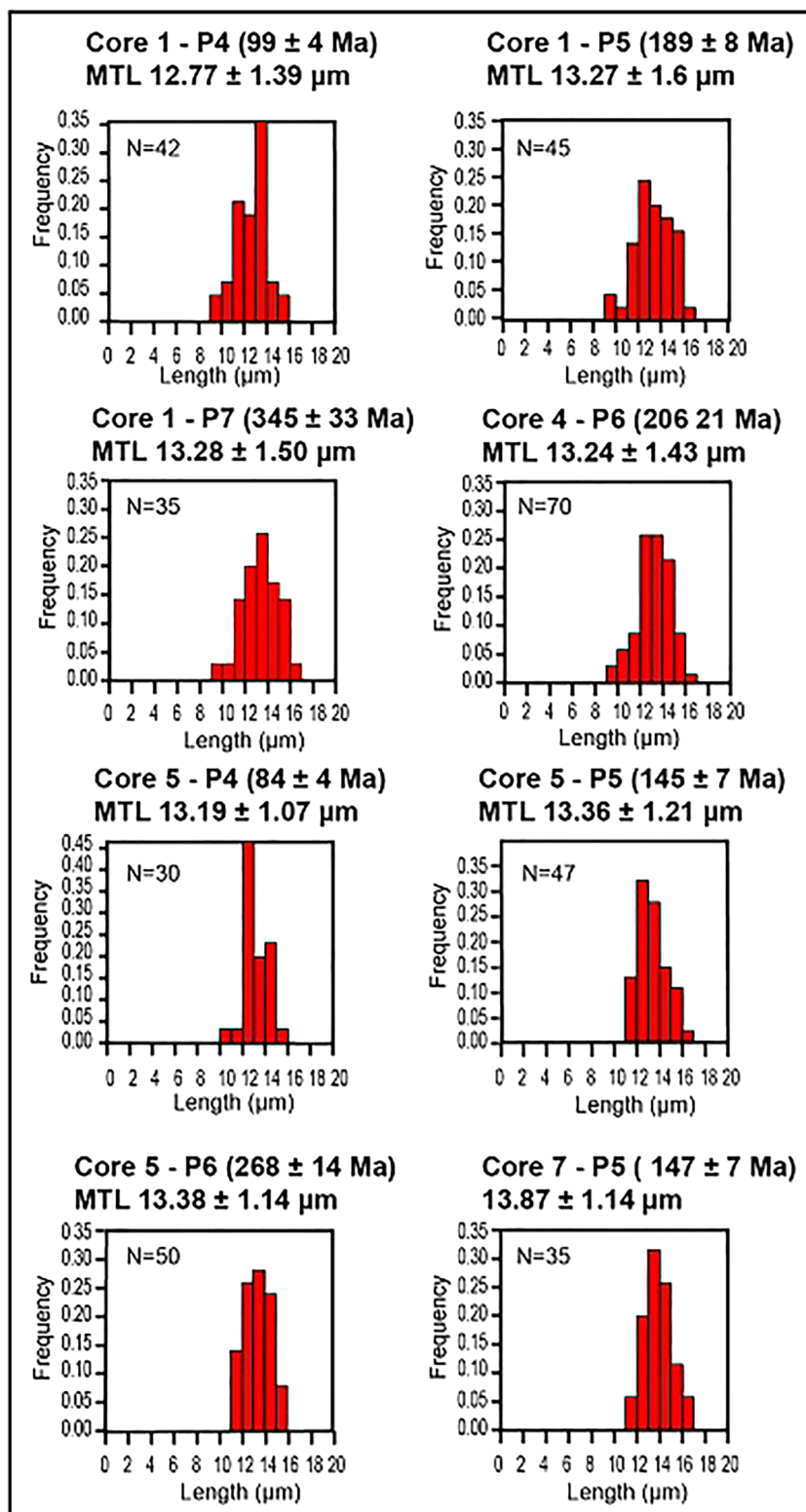


Figure 6. Fission track confined length distributions (c axis corrected). Value of mean track length is shown with standard deviation.

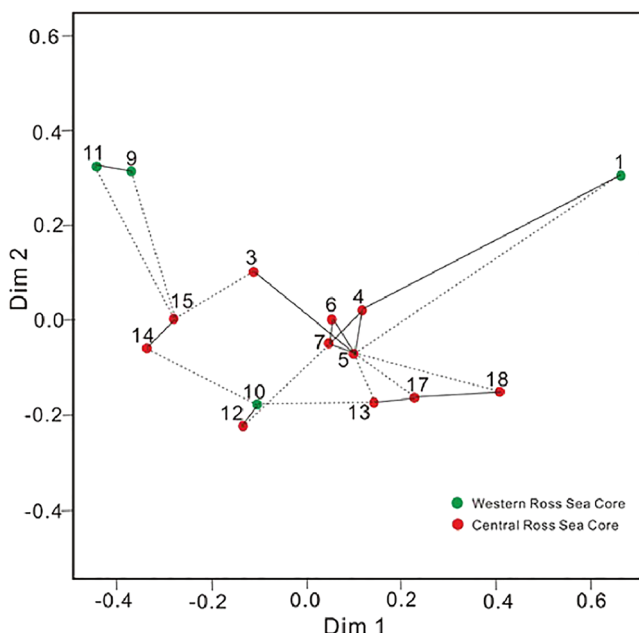


Figure 7. Multidimensional scaling plot showing relative statistical similarity. Samples 2 and 8 yield too few grains and have been not included. “Similar” samples cluster closely together, and “dissimilar” samples plot far apart (Vermeesch, 2013).

In fact, source of bias could be represented by vulnerability of grain age distribution to hydraulic sorting effects and the mineral fertility of the source rock (Malusà & Garzanti, 2019).

The youngest age population (P1) comprises grains younger than 21 Ma. Generally, this age population is poorly represented in our data set. However, it appears clearly in cores 3 and 5 located in the CRS and in core 9 close to McMurdo Island in the WRS, although some grains are present also in piston cores 13 and 14.

Grains belonging to population P2 range from 21 to 46 Ma, and they are widespread present in many piston cores from the CRS (piston cores 2–7 and 15) and also in piston core 11, which is close to the WRS. It is noteworthy the absence of the P2 population in the piston core 1, collected close to the Victoria Land coast.

There are no clear trends in the abundance of grains belonging to populations P3 (53 – 75 Ma), P4 (84 – 100 Ma), P5 (112 – 190 Ma), and P6 (222 – 270 Ma). Generally, grains in these age ranges are much more abundant than other populations. P7 groups the oldest grains, with ages higher than 270 Ma. This age population appears meaningfully in piston cores 1, 4, 5, and 7, which are located in the CRS and the WRS. The number of grains is usually quite low with the exception of sample 1.

Figure 7 shows a graphical representation of the statistical similarity among the samples obtained by the multidimensional scaling method (Vermesch, 2013), where the solid lines mark the closest neighbors and dashed lines the second closest neighbors. Detrital data define different groups with most samples (4-5-6-7) from the CRS that cluster closely together. Besides, sample 1 (East Antarctic coast) and samples 9–11 (WRS) both plot far from the other samples and from each other, pointing to a peculiar detrital age signature (Figure 7). Samples 4-5-6-7 are the closest neighbors. It is noteworthy that the age distributions of these four piston cores show the largest age range among all piston cores. They yield four to six age populations with no grains belonging to the P1 age population and similar grain abundance in the populations P2 and P4. They are all located in the eastern flank of Central High (Ross Bank) in the CRS. Samples 13 – 17 show most grains with an age of about 130 Ma (P5) and a further population P3 with an age of about 50 – 60 Ma. These two piston cores are both in the CRS and not far from the continental shelf. The similarity of samples 10 – 12 is given by three main age populations at 60 Ma (P3), 90 Ma (P4), and 150 Ma (P5). They are located a bit far from each other, but at the similar latitude and very close to the border of the present Ross Ice Shelf (actually sample 10 is below the shelf).

4. Results and Data Interpretation

At least 40 grains have been measured in 23 samples, whereas only 17 to 37 grains could be measured in the remaining 6 samples. Samples analyzed from the same piston cores do not show significant variability with depth. The same observation was done by Licht et al. (2014) on U-Pb age distributions. Therefore, considering also that the lack of high-resolution chronology within the till and thus any time-transgressive analysis of flow changes is not possible and that the number of available grains is usually very low given the scarcity of sampled material, we merged age data of different samples from the same piston cores in order to increase the robustness of statistics. For example, piston core 1 included five samples with different core length ranges: 25 – 32, 102 – 107, 187 – 192, 242 – 247, and 297 – 302 cm (Table 2). As a whole, the single grain ages cover a large range, spanning from 7.9 to 539.3 Ma, and all samples show overdispersion of ages relative to values predicted for standard Poissonian variation for a single age component. The youngest grains (AFT ages < ~20 Ma), those with AFT age ~30 – ~40 Ma, and the oldest population grains have been revealed as the most significant in terms of source signature, as already described in literature (Li et al., 2019; Olivetti et al., 2013; Perotti et al., 2017; Zattin et al., 2012, 2014). However, to facilitate a comparison among AFT distributions, we identified seven different age populations, although not all of them are present in all the samples (Table 2 and Figure 4). We stress here the fact that any interpretation based on relative proportion among grain age populations must be done with cau-

5. Discussion

5.1. Identification of EAIS and WAIS Sources

The large range of individual grain ages and the lack of systematic trends across the Ross Sea indicate the presence of multiple sources with probably complex exhumation histories. Therefore, our major task was the finding of key data able to give an unambiguous signature to EAIS and WAIS provenance.

A first clue is given by the youngest age population ($P1 < 21$ Ma) in our fission track age data set (Table 2 and Figure 4). Such young grains are also present in data sets detected on offshore drill holes such as CIROS-2 and ANDRILL and were interpreted as related to the widespread Cenozoic volcanic event in the WRS (Zattin et al., 2012). On the contrary, these ages are not present in the fission track detrital distributions in the ERS (Perotti et al., 2017) and in the U-Pb detrital zircon signature of West Antarctic sites (Licht et al., 2014). Actually, some volcanic centers exist in West Antarctica, but their contribution to the detritus that is flowing into the eastern Ross Sea is very minor (Anderson et al., 1992; Licht et al., 2005; Perotti et al., 2017). However, it is possible that rare volcanic clasts could derive from the unexposed volcanic centers at present under the ice sheet in western Marie Byrd Land (Behrendt et al., 1995, 2004; Ferraccioli et al., 2002; Luyendyk et al., 2003; Perotti et al., 2017). It is possible that erosion of these volcanic centers occurred earlier than the LGM (Licht et al., 2005). Therefore, we suggest that where the $P1$ population is present, a WAIS source can be reasonably excluded. In East Antarctica, except of course the surroundings of the McMurdo Volcanic Province, volcanic clasts have been detected in the Royal Society Range foothills (Perotti et al., 2018), the Dry Valleys (Ehrmann & Polozek, 1999; Kyle, 1981, 1990; Marchant et al., 1996; Sandroni & Talarico, 2006), and, more to the north, along the northern Victoria Land (Müller et al., 1991; Rocchi et al., 2002). Considering the location of sample 9, in which $P1$ clasts are abundant, we speculate that the youngest grains in this sample are derived from McMurdo Volcanic Group. Less obvious is the explanation for $P1$ grains in samples 3 and 5, which are located in the CRS, thus quite far from the McMurdo volcanic edifices, taking also in account that the young grains are absent in the nearby piston cores. Based on the location of existing McMurdo volcanic outcrops, Licht et al. (2005), given the widespread presence of volcanic glasses in samples from the WRS, suppose a transport distance from a few tens of kilometers to over 100 km. However, it is also possible that some apatites are derived from volcanic sources located south of the McMurdo region but at present below the ice. This hypothesis was already mentioned by Zattin et al. (2012) to explain the presence of volcanic detritus in the drill hole AND-2A. More broadly, the presence of $P1$ apatites, clearly of volcanic origin, represents the signature for a west derived source, which is related to evolution of East Antarctica. In other words, the presence of these grains in samples 3 and 5 and their absence in samples closer to West Antarctica (Perotti et al., 2017) suggests that the area of Central High was reached by EAIS-derived flows. This view is supported by the distribution of $P7$ apatites, which is older than 278 Ma. They appear meaningfully in piston cores 1, 4, 5, 7, which are located in the CRS and the WRS. Generally, exhumation ages detected on bedrock samples from East Antarctica are older than those from West Antarctica (Figure 3). For example, Fitzgerald (1994) detected AFT ages of 253 – 339 Ma in the Miller Range along the TAM, whereas apatite fission track ages in the Marie Byrd Land are Cretaceous or younger (Adams et al., 1995; Lisker & Olesch, 1998; Spiegel et al., 2016; Zundel et al., 2019). Moreover, published detrital fission track ages from piston cores located in the ERS (therefore sourced certainly from West Antarctica) are all younger than 222 Ma (Perotti et al., 2017). On the contrary, sparse grains with ages older than 200 Ma have been detected offshore the TAM in the CRP, CIROS2, and Andrill wells (Olivetti et al., 2013, 2015; Zattin et al., 2010, 2012). We therefore infer that the presence of populations $P1$ and $P7$ may represent a significant signature of an East Antarctic source.

We rule out the possibility that $P1$ ages are not related to magmatic cooling but to exhumation. In fact, although extensional tectonics has been proved along the margins of the West Antarctic Rift System during the Neogene (Cooper & Davey, 1985; LeMasurier, 2008), apatite fission track bedrock ages younger than about 20 Ma have been never found. The youngest exhumation event has been described by Spiegel et al. (2016) in eastern Marie Byrd Land at about 20 Ma.

On the contrary, the appearance of $P2$ apatites (28 to 46 Ma) (Table 2 and Figure 4) is a clear signal of Oligocene exhumation in the source regions. These grains are well represented both in the CRS and the WRS. Detrital apatite fission track ages ranging from 30 to 40 Ma have been already detected offshore the central TAM, although in older sediments (Li et al., 2019; Zattin et al., 2010, 2012). They derive from

erosion of exhumed blocks exposed along the TAM front as they match exhumation phases detected on bedrock samples (Fitzgerald, 2002; Olivetti et al., 2015, 2018; Zattin et al., 2014). Actually, such fission track ages are rare in the Dry Valleys (Fitzgerald et al., 2006; Gleadow & Fitzgerald, 1987) and Granite Harbor region (Fitzgerald, 1992), but they have been detected in the Royal Society Range (Olivetti et al., 2018) and are also abundant to the south, between the Skelton and Byrd Glaciers (Huerta et al., 2011; Zattin et al., 2014) as well as much farther (600 km) to the south (Fitzgerald, 1994; Fitzgerald & Stump, 1997; Miller et al., 2010; Stump & Fitzgerald, 1992). However, apatite fission track data by Perotti et al. (2018) also show samples in the ERS (P3, P4, P6, P8, and P9 in Figure 1), possibly derived from West Antarctica, that yield grains with ages from 30 to 40 Ma. A further support to an Oligocene exhumation phase derives by results obtained by thermal modeling, as described in the following section. In fact, a presence of a marked increase in cooling rates is visible in most of our simulations. It is noteworthy that the presence of this cooling event is irrespective of the fission track age of the modeled sample.

A comparison of the AFT population age of LGM deposit with Miocene to Pleistocene sediments of CIROS, CRP and ANDRILL shows a relative abundance of grain ages older than 100 Ma with respect to younger grain. Following the quite consistent age elevation distribution of the AFT along the TAM (i.e., the occurrence of young AFT ages at low elevation), we can associate the abundance of old AFT ages with the higher elevation of the Ross Ice Sheet and relative outlet glaciers during the LGM (e.g., Bromley et al., 2010). In other words, the high elevation of the surface glaciers cross cutting the TAM supported erosion of high elevated rocks.

5.2. Thermal Modeling of Detrital Populations

Thermal modeling in detrital samples is not a usual procedure as it is based on the assumption that all the grains with the same age derive from the same source rock. Sources of bias can be related to analytical procedures (e.g., the difficulty to assign the measured length to a proper age population) or to unambiguous identification of geological constraints. To avoid any overinterpretation, we simply compare our data with exemplifying thermal histories derived from literature for different areas around the Ross Sea embayment. Such a forward modeling procedure was done with the HeFty software (Ketcham, 2005).

We focus on populations P4, P5, and P6, for which an unambiguous provenance was not possible by simple comparison with bedrock ages. The age of the P4 population suggests a possible source region where a Late Cretaceous exhumation phase is preserved today. Several areas around Ross Sea embayment show these ages, interpreted in many study as the onset of West Antarctica and East Antarctica extension and spreading between Antarctica and Australia (Goodge, 2020). These samples are usually confined in the inland portion of the TAM and at high elevation, while in Marie Byrd Land they are common but associated with rapid cooling (and long mean track length) that is not consistent with our data, making the Marie Byrd provenance highly unlike (Figure 8a). Thermal history of some bedrock samples from southern and central TAM (Scott Glacier and Beardmore Glacier region) shows age and mean track length consistent with our P4 data of core 5. These data support the occurrence of glacial flow that during or just after LGM transported sediment from southern and central TAM to the central Ross Sea.

The mean track length of the P4 population in core 1 is shorter than the mean track length of the P4 population in core 5 and of bedrock samples from the southern and central TAM. Even accounting for data uncertainty beyond the standard deviation, the mean track length and age of the P4 population in core 1 seem consistent with the fission track data from the high elevated samples of the Dry Valleys (Fitzgerald, 1992; Gleadow & Fitzgerald, 1987). Thermal modeling of Dry Valleys samples has never been performed; therefore, any comparison is purely speculative. A simple comparison of P4 of core 1 with AFT ages from Terra Nova Bay region (Balestrieri et al., 1997, 1999; Fitzgerald & Gleadow, 1988; Lisker, 1996; Prenzel et al., 2014, 2018; Storti et al., 2008) does not allow to rule out a provenance from this region and a glacial flow coming from the northern Victoria Land.

The comparison of the possible thermal history of P5 population with bedrock cooling is made difficult by the few bedrock samples recording Early Cretaceous ages. Scott Glacier, Beardmore Glacier, Dry Valleys, and Terra Nova Bay regions show some samples with comparable AFT ages (Fitzgerald, 2002), although their thermal histories are sometime uncertain. A thermal history with a trend similar to what proposed for the Scott Glacier and already tested for the P4 core 5 seems consistent, although at different

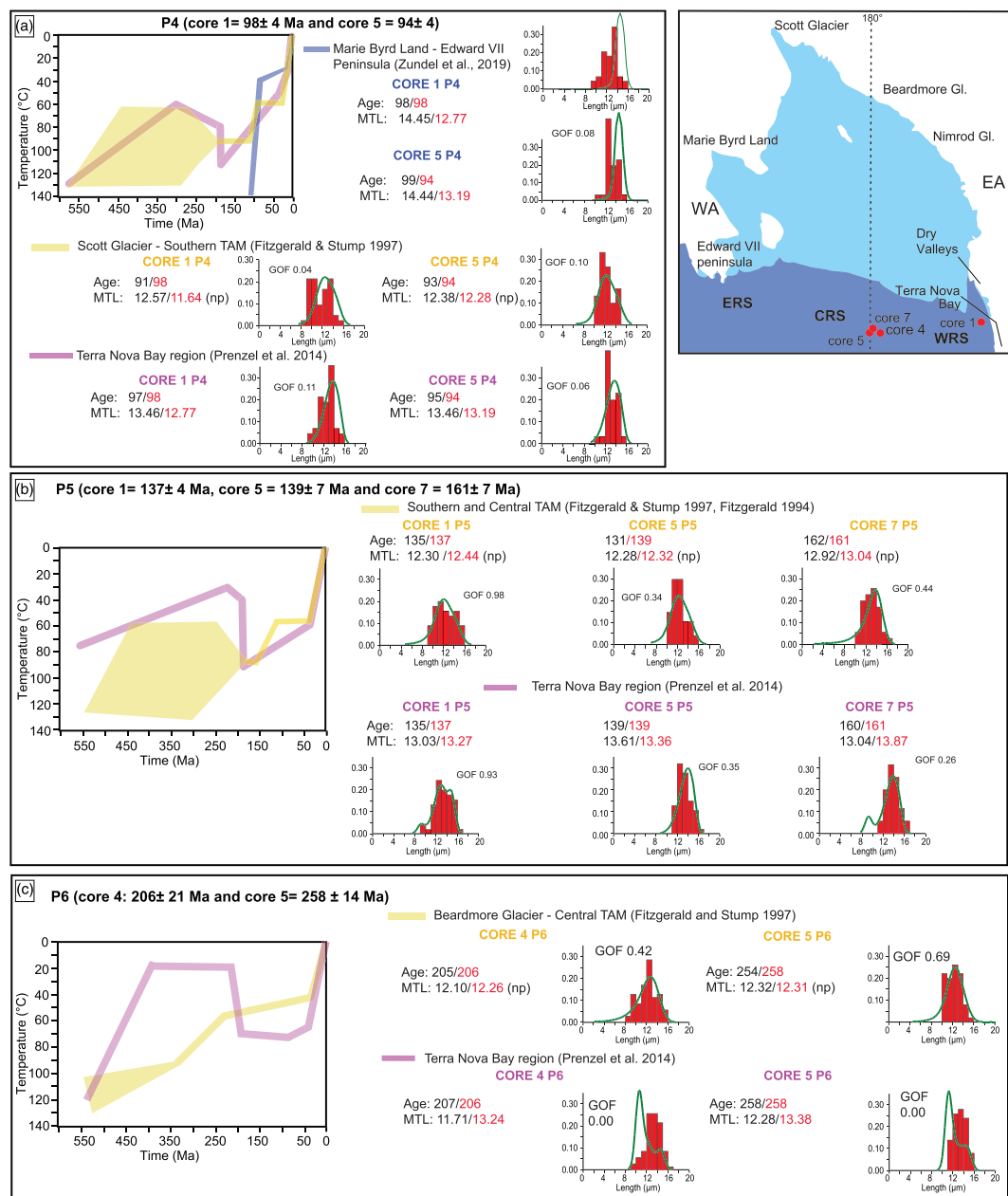


Figure 8. Forward thermal modeling of AFT detrital populations obtained by HeFTy software (Ketcham, 2005). The figure shows a comparison between ages and track length distribution obtained by forward modeling (in black) with observed data (in red) of detrital population P4 (a), P5 (b), and P6 (c). Coupled with the age and MTL (mean track length) modeled versus observed, we show the observed track length distribution histogram with the modeled density curve (in green). GOF (goodness of fit) gives an indication about the fit between observed and predicted data (values close to 1 are best) as it reveals the probability of failing the null hypothesis that the model and data are different. Modeled data have been derived from literature for different location along the TAM to identify possible provenance area. Three thermal histories have been investigated: a rapid Cretaceous cooling representative of Marie Byrd Land samples (for the P4 only), a nearly constant cooling with a Cretaceous cooling event representative of some samples from southern and central TAM and the a more complex path with a Paleozoic cooling followed by a burial and a further cooling.

temperature ranges, with P5, providing further evidence for a southern central TAM provenance for the Central Ross Sea sediment. The comparison between the exhumation ages of the Terra Nova Bay region (Prenzel et al., 2014) with the P5 data of core 1 shows a good fit suggesting a possible provenance from northern Victoria Land.

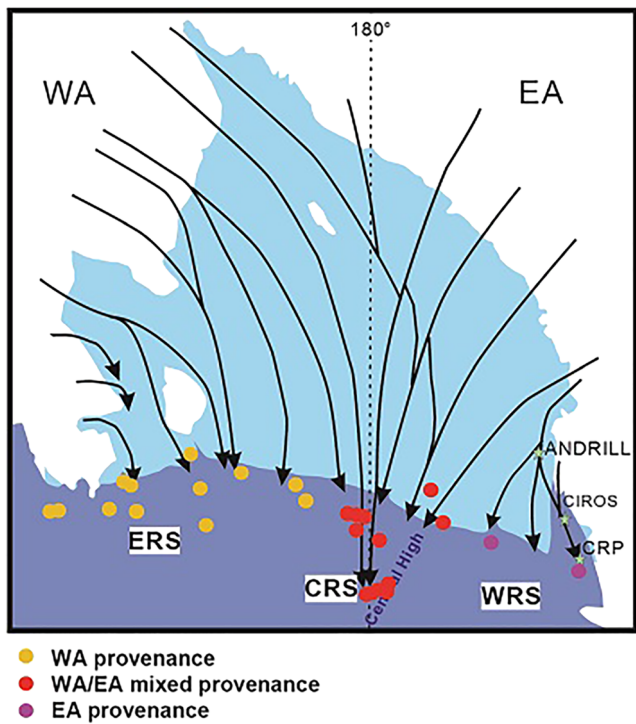


Figure 9. Ice flow lines of the Ross Sea ice sheet during the LGM based on apatite fission track signatures and literature data from Anderson et al. (2014), Li et al. (2019), Licht et al. (2005, 2014), Perotti et al. (2017), and Zattin et al. (2010, 2012).

noteworthy that despite different interpretations, all these paths are characterized to yield an increase of cooling rates in the Cenozoic, and specifically in the Oligocene.

The whole data set suggests therefore that an Oligocene increase in cooling rate is recurrent. At a first glance, this increase can be associated to a continental-scale erosion related to the renewed activity of the West Antarctic Rift System (Cande et al., 2000; Prenzel et al., 2013, 2014; Spiegel et al., 2016). According to the general topography of the TAM, bedrocks with Cenozoic AFT ages are mostly limited to low elevation areas (see Lisker & Laufer, 2013, for a discussion about relationships between topography and occurrence of pre-Cretaceous ages) and thus along the rift shoulder uplifts. Actually, LeMasurier and Landis (1996) document the formation of erosion surfaces in West Antarctica, related to a period of tectonic quiescence between 70 and 50 Ma, with a renewed relief formation since 30 Ma; since then, uplift and/or erosion was restricted to central Marie Byrd Land. Along the TAM, the AFT ages move rapidly from the coast to inland region toward ages older than approximately 50 Ma, until approximately 200 Ma (Fitzgerald, 2002). As suggested by thermal modeling, which shows some increase of cooling rates during the Cenozoic also for inland areas, it appears that these regions were affected by enhanced erosion, with the removal of approximately 1 km of crust in the last 50 Ma.

The extent of this erosional event, not associated to a focused deformation along the TAM front, could be the evidence of a climatic signal due to the Cenozoic general descent into icehouse condition that for East Antarctica is dated at approximately 35 Ma (Coxall et al., 2005). The estimate of erosion is not far from what has been calculated by the most recent numerical ice sheet models that predict a very low erosion of inland areas in East Antarctica although the establishment of an extensive ice sheet is a gradual event and major ice growth did not occur until approximately 26 Ma (Paxman et al., 2019; Pollard & DeConto, 2020).

5.3. Implications on Ice Flow Dynamics

Given the widespread presence of P2 apatites in most of the samples, it is noteworthy their absence in the piston core 1 (Table 2, Figure 3), located close to East Antarctica coast. As already mentioned, on the basis

P6 population is not affected by the thermal event of the Ferrar volcanism nor by the later sedimentary burial as hypothesized by Lisker and Laufer (2013) for the Victoria Land. P6 population occurred in four only cores, mostly from the central Ross Sea, showing a large spread in the central age among the cores. Among the bedrock samples, AFT ages in the 200–270 Ma range are rare: A group of ages in the range between 250 and 300 Ma were dated along a vertical profile from the Miller Range (Fitzgerald, 1994), between Beardmore and Nimrod glacier (Figures 2 and 3). These ages were interpreted as produced by cooling during Carboniferous-Permian, followed by a long permanence in the uppermost part of the temperature range of partial annealing until a last cooling event during the Cenozoic. This thermal history is well consistent with the age and mean track length of P6 of core 5 (Figure 8). Although population P6 of core 4 is younger, it is still consistent with that thermal history (Figure 8); difference in age could be related to a possible provenance from a lower crustal level.

Along the TAM, similar ages have been found on the uppermost samples from the Terra Nova Bay region (Prenzel et al., 2014, 2018). Although the ages are comparable, the mean track length are different, and the thermal history proposed for Terra Nova Bay region seems incompatible with the long mean track length of our P6. However, it is noteworthy that Prenzel et al. (2014, 2018) were able to measure a significant number of track lengths on two samples only, making any consideration on thermal history of this region quite weak.

As a whole, these data suggest that apatites from CRS are compatible with thermal histories that have been derived from samples from central TAM, in an area comprised between the Nimrod and the Scott Glaciers. It is

of the multidimensional scaling statistics (Figure 7), site 1 yields a very peculiar distribution of single grain ages, clearly different from the samples collected in the CRS (piston cores 4-5-6-7) and from those more to the east. Nearby site 1 (55-km south), single grain ages of about 30 Ma had been detected on samples from Pliocene sediments in the offshore drill hole CRP (Olivetti et al., 2013). Furthermore, similar ages are present in the Plio-Pleistocene samples from the CIROS-2 well (Li et al., 2019). In general, literature agrees on a northward ice flow along the coast of TAM, which was able to bring sediments from the outlet glaciers of East Antarctica (Olivetti et al., 2013, 2015; Zattin et al., 2010, 2012). Our data demonstrate that sediments transported by the ice flow from the south did not reach the site 1 (Figure 9), and therefore, the supply is mainly from the local East Antarctica outlet glaciers. However, although maximum ice sheet advance reached site 1, as demonstrated by Anderson et al. (2014), the interplay between west and south derived ice flow was complex, with one prevailing on the other, during the ice retreat after the LGM. Considering the fission track populations P1 and P7 (Table 2 and Figure 4) as marker signals for a provenance from East Antarctica as discussed above and the inferences obtained by forward modeling, the Central High seems to represent a major divide between EAIS and WAIS flows (Figure 9). A similar conclusion was suggested by Denton and Hughes (2000), Licht and Fastook (1998), and Licht et al. (2005, 2014) on the basis of different data sets. From a topographic point of view, the convergence of ice is marked by two merging sets of megascale glacial lineation detected by multibeam swath bathymetry (Anderson et al., 2014; Shipp et al., 1999; Tinto et al., 2019). These results are also broadly consistent with the paleoflows estimated by numerical modeling by Golledge et al. (2012).

6. Conclusions

This work shows that detrital apatite fission track analysis can be a valuable tool to reconstruct the sedimentary provenance pattern of a region where bedrock geology is poorly known. In fact, the samples here analyzed offer a picture of the ice flow dynamics after the LGM in the Ross embayment but, at the same time, capture the signals given by differential exhumation of East and West Antarctica.

The overall framework derived from statistical analysis of age groups indicates a complex exhumation of the TAM and the regions belonging to West Antarctica starting at least since the Jurassic. However, thermal modeling and the presence of apatites with cooling ages of about 30–40 Ma suggests that an Oligocene exhumation event, associated to the last phases of the West Antarctic Rift System, is widespread all along the margins of the Ross Sea, therefore affecting both West and East Antarctica. Possible further tectonics related to the rift during the Neogene produced, if present, less than 2 km of exhumation.

The presence of key marker apatites (e.g., younger than 20 Ma or older than 230 Ma) and forward modeling of thermal histories derived from literature bedrock ages allows to identify the Central High as a major ice flow divide. West of the Central High, the ice flow is from East Antarctica, with general northward trend but with local flows from outlet glaciers, especially during ice sheet retreat phases. East of the Central High, sediments derived mainly by West Antarctica, with only minor contributions from the southernmost portion of the TAM and the lack of any significant input from the inner Marie Bird Land.

Data Availability Statement

Data of this study can be accessed through open access Research Data Unipd repository (<http://researchdata.cab.unipd.it/id/eprint/162>).

Acknowledgments

This version of the paper greatly benefited from the accurate and thoughtful revisions of Frank Lisker, Gordon Bromley, and of the Associate Editor. We thank the Antarctica Research Facility at Florida State University for access to the core repository. We thank S. Boesso for assistance in sample processing. This work was supported by China Scholarship Council (CSC) (no. 201606410071) and PNRA (PNRA16_00263 coordinated by V. Olivetti).

References

- Adams, C. J. (1986). Geochronological studies of the Swanson Formation of Marie Byrd Land, West Antarctica, and correlation with northern Victoria Land, East Antarctica, and South Island, New Zealand. *New Zealand Journal of Geology and Geophysics*, 29(3), 345–358. <https://doi.org/10.1080/00288306.1986.10422157>
- Adams, R. M., Fleming, R. A., Chang, C. C., McCarl, B. A., & Rosenzweig, C. (1995). A reassessment of the economic effects of global climate change on U.S. agriculture. *Climatic Change*, 30, 147–167. <https://doi.org/10.1007/bf01091839>
- Allibone, A. H., Cox, S. C., Graham, I. J., Smillie, R. W., Johnstone, R. D., Ellery, S. G., & Palmer, K. (1993). Granitoids of the Dry Valleys area, southern Victoria Land, Antarctica: Plutons, field relationships, and isotopic dating. *New Zealand Journal of Geology and Geophysics*, 36(3), 281–297. <https://doi.org/10.1080/00288306.1993.9514576>
- Anderson, J. B., Conway, H., Bart, P. J., Witus, A. E., Greenwood, S. L., McKay, R. M., et al. (2014). Ross Sea paleo-ice sheet drainage and deglacial history during and since the LGM. *Quaternary Science Reviews*, 100, 31–54. <https://doi.org/10.1016/j.quascirev.2013.08.020>

- Anderson, J. B., Shipp, S. S., Bartek, L. R., & Reid, D. E. (1992). Evidence for a grounded ice sheet on the Ross Sea continental shelf during the late Pleistocene and preliminary paleodrainage reconstruction. *AGU Antarctic Research Series*, 57, 39–62. <https://doi.org/10.1029/AR057p0039>
- Balestrieri, M. L., Bigazzi, G., & Ghezzo, C. (1997). Uplift-denudation of the Transantarctic Mountains between the David and the Mariner glaciers, northern Victoria Land (Antarctica); constraints by apatite fission-track analysis. In C. A. Ricci (Ed.), *The Antarctic Region: Geological Evolution and Processes* (pp. 547–554). Siena: Terra Antarctica Publication.
- Balestrieri, M. L., Bigazzi, G., & Ghezzo, C. (1999). The Transantarctic Mountains: A natural laboratory for apatite fission-track analysis. Results from Italian Antarctic expeditions. *Radiation Measurements*, 31, 621–626. [https://doi.org/10.1016/S1350-4487\(99\)00154-7](https://doi.org/10.1016/S1350-4487(99)00154-7)
- Balshaw, K. M. (1980). *Antarctic glacial chronology reflected in the Oligocene through Pliocene sedimentary section in the Ross Sea* (PhD thesis, pp. 1–140). Rice University.
- Barrett, P. J. (1991). The Devonian to Triassic Beacon Supergroup of the Transantarctic Mountains and correlatives in other parts of America. In R. J. Tingey (Ed.), *The Geology of Antarctica, Monographs on Geology and Geophysics* (Vol. 17, pp. 120–152). Oxford, U.K.: Oxford University Press.
- Bart, P. J., & Cone, A. N. (2012). Early stall of West Antarctic Ice Sheet advance on the eastern Ross Sea middle shelf followed by retreat at 27, 500 ^{14}C yr BP. *Palaeogeography, Palaeoclimatology, Palaeoecology*, 335–336, 52–60. <https://doi.org/10.1016/j.palaeo.2011.08.007>
- Behrendt, J., Finn, C., Blankenship, D. D., Morse, D., & Bell, R. (2004). Do the volcanic rocks erupted in the West Antarctic rift system beneath the West Antarctic Ice Sheet (WAIS), interpreted from aeromagnetic surveys, define a large igneous province? Paper presented at AGU Fall Meeting, San Francisco, USA.
- Behrendt, J. C., Donald, D., Blankenship, D. D., & Alan, K. C. (1995). Glacial removal of late Cenozoic subglacially emplaced volcanic edifices by the West Antarctic ice sheet. *Geology*, 23(12), 1111–1114. [https://doi.org/10.1130/0091-7613\(1995\)023%3C1111:GROLCS%3E2.3.CO;2](https://doi.org/10.1130/0091-7613(1995)023%3C1111:GROLCS%3E2.3.CO;2)
- Bradshaw, J. D., Andrews, P. B., & Field, B. D. (1983). Swanson formation and related rocks of Marie Byrd Land and a comparison with the Robertson Bay Group of northern Victoria Land. *Antarctic Earth Science*, 1982, 274–279.
- Brand, J. F. (1979). *Low grade metamorphic rocks of the Ruppert and Hobbs coasts of Marie Byrd Land, Antarctica* (MSc thesis, pp. 1–49). Lubbock, TX: Texas Tech University.
- Bromley, G. R., Hall, B. L., Stone, J. O., Conway, H., & Todd, C. E. (2010). Late Cenozoic deposits at Reedy Glacier, Transantarctic mountains: Implications for former thickness of the West Antarctic Ice Sheet. *Quaternary Science Reviews*, 29(3–4), 384–398. <https://doi.org/10.1016/j.quascirev.2009.07.001>
- Burtner, R. L., Nigrini, A., & Donelick, R. A. (1994). Thermochronology of Lower Cretaceous source rocks in the Idaho-Wyoming Thrust Belt. *Bulletin of the American Association of Petroleum Geologists*, 78, 1613–1636. <https://doi.org/10.1306/a25ff233-171b-11d7-8645000102c1865d>
- Bushnell, V. C., & Craddock, C. (1970). Geologic maps of Antarctica. *Antarctic Map Folio Series*, 12(plate 23).
- Cande, S., Stock, J., Müller, D., & Ishihara, T. (2000). Cenozoic motion between East and West Antarctica. *Nature*, 404, 145–150. <https://doi.org/10.1038/35004501>
- Cook, Y. A., & Craw, D. (2002). Neoproterozoic structural slices in the Ross Orogen, Skelton Glacier area, South Victoria Land, Antarctica. *New Zealand Journal of Geology and Geophysics*, 45(1), 133–143. <https://doi.org/10.1080/00288306.2002.9514965>
- Cooper, A. K., & Davey, F. J. (1985). Episodic rifting of Phanerozoic rocks in the Victoria Land basin, western Ross Sea, Antarctica. *Science*, 229, 1085–1087. <https://doi.org/10.1126/science.229.4718.1085>
- Coxall, H. K., Wilson, P. A., Pálike, H., Lear, C. H., & Backman, J. (2005). Rapid stepwise onset of Antarctic glaciation and deeper calcite compensation in the Pacific Ocean. *Nature*, 433(7021), 53–57. <https://doi.org/10.1038/nature03135>
- Denton, G. H., & Hughes, T. J. (2000). Reconstruction of the Ross Ice drainage system, Antarctica, at the last glacial maximum. *Geografiska Annaler*, 82(2–3), 143–166. <https://doi.org/10.1111/j.0435-3676.2000.00120.x>
- Dietze, M., Kreutzer, S., Burov, C., Fuchs, M., Fischer, M., & Schmidt, C. (2016). The abanico plot: Visualizing chronometric data with individual standard errors. *Quaternary Geochronology*, 31, 12–18. <https://doi.org/10.1016/j.quageo.2015.09.003>
- Dolan, A. M., de Boer, B., Bernales, J., Hill, D. J., & Haywood, A. M. (2018). High climate model dependency of Pliocene Antarctic ice-sheet predictions. *Nature Communications*, 9, 2799. <https://doi.org/10.1038/s41467-018-05179-4>
- Domack, E. W., Jacobson, E. A., Shipp, S., & Anderson, J. B. (1999). Late Pleistocene-Holocene retreat of the West Antarctic Ice Sheet in the Ross Sea: Part 2—Sedimentologic and stratigraphic signature. *Bulletin of the Geological Society of America*, 111(10), 1517–1536. [https://doi.org/10.1130/0016-7606\(1999\)111%3C1517:LPHROT%3E2.3.CO;2](https://doi.org/10.1130/0016-7606(1999)111%3C1517:LPHROT%3E2.3.CO;2)
- Donelick, R. A. (1993). Apatite etching characteristics versus chemical composition. *Nuclear Tracks and Radiation Measurements*, 21(4), 604. [https://doi.org/10.1016/1359-0189\(93\)90241-z](https://doi.org/10.1016/1359-0189(93)90241-z)
- Dunbar, R. B., Anderson, J. B., Domack, E. W., & Jacobs, S. S. (1985). Oceanographic influences on sedimentation along the Antarctic continental shelf: Oceanology of the Antarctic Continental Shelf. *American Geophysical Union Antarctic Research Series*, 43, 291–312. <https://doi.org/10.1029/AR043p0291>
- Ehrmann, W., & Polozek, K. (1999). The heavy mineral record in the Pliocene to Quaternary sediments of the CIROS-2 drill core, McMurdo Sound. *Antarctica Sedimentary Geology*, 128, 223–244. [https://doi.org/10.1016/S0037-0738\(99\)00071-8](https://doi.org/10.1016/S0037-0738(99)00071-8)
- Elliot, D. H., Fanning, C. M., & Hulett, S. R. W. (2015). Age provinces in the Antarctic craton: Evidence from detrital zircons in Permian strata from the Beardmore Glacier region, Antarctica. *Gondwana Research*, 28, 152–164. <https://doi.org/10.1016/j.gr.2014.03.013>
- Elliot, D. H., & Fleming, T. H. (2008). Physical volcanology and geological relationships of the Jurassic Ferrar Large Igneous Province, Antarctica. *Journal of Volcanology and Geothermal Research*, 172(1–2), 20–37. <https://doi.org/10.1016/j.jvolgeores.2006.02.016>
- Farmer, G. L., Barber, D., & Andrews, J. (2003). Provenance of Late Quaternary ice-proximal sediments in the North Atlantic: Nd, Sr and Pb isotopic evidence. *Earth and Planetary Science Letters* Version 1, 209, 227–243. [https://doi.org/10.1016/S0012-821X\(03\)00068-2](https://doi.org/10.1016/S0012-821X(03)00068-2)
- Farmer, G. L., & Licht, K. J. (2016). Generation and fate of glacial sediments in the central Transantarctic Mountains based on radiogenic isotopes and implications for reconstructing past ice dynamics. *Quaternary Science Reviews*, 150, 98–109. <https://doi.org/10.1016/j.quascirev.2016.08.002>
- Farmer, G. L., Licht, K. J., Swope, R. J., & Andrews, J. (2006). Isotopic constraints on the provenance of fine-grained sediment in LGM tills from the Ross Embayment, Antarctica. *Earth and Planetary Science Letters*, 249(1–2), 90–107. <https://doi.org/10.1016/j.epsl.2006.06.044>
- Faure, G., & Mensing, T. M. (1993). K-Ar dates and paleomagnetic evidence for Cretaceous alteration of Mesozoic basaltic lava flows, Mesa Range, northern Victoria Land, Antarctica. *Chemistry Geology*, 109, 305–315. [https://doi.org/10.1016/0009-2541\(93\)90077-V](https://doi.org/10.1016/0009-2541(93)90077-V)
- Ferraccioli, F., Bozzo, E., & Armadillo, E. (2002). A high-resolution aeromagnetic field test in Friuli: Towards developing remote location of buried ferro-magnetic objects. *Annals of Geophysics*, 45, 219–232. <https://doi.org/10.4401/ag-3503>

- Findlay, S., & Meyer, J. L. (1984). Significance of bacterial biomass and production as an organic carbon source in lotic detrital systems. *Bulletin of Marine Science*, 35, 318–325.
- Fitzgerald, P. G. (1992). The Transantarctic Mountains of southern Victoria Land: The application of apatite fission track analysis to a rift shoulder uplift. *Tectonics*, 11(3), 634–662. <https://doi.org/10.1029/91TC02495>
- Fitzgerald, P. G. (1994). Thermochronologic constraints on post-Paleozoic tectonic evolution of the central Transantarctic Mountains, Antarctica. *Tectonics*, 13, 818–836. <https://doi.org/10.1029/94TC00595>
- Fitzgerald, P. G. (2002). Tectonics and landscape evolution of the Antarctic plate since the breakup of Gondwana, with an emphasis on the West Antarctic Rift System and the Transantarctic Mountains. *The Royal Society of New Zealand bulletin*, 35, 453–469.
- Fitzgerald, P. G., & Baldwin, S. L. (2007). Thermochronologic constraints on Jurassic rift flank denudation in the Thiel Mountains, Antarctica. In A. Cooper, C. Raymond, & the 10th ISAES Editorial Team (Eds.), *Antarctica: A keystone in a changing world—Online Proceedings for the 10th International Symposium on Antarctic Earth Sciences, Open File Report, 2007–1047* (Vol. 044, pp. 1–4). Santa Barbara, CA: U.S. Geological Survey. <https://doi.org/10.3133/of2007-1047.srp044>
- Fitzgerald, P. G., Baldwin, S. L., Webb, L. E., & O'Sullivan, P. B. (2006). Interpretation of (U-Th)/He single grain ages from slowly cooled crustal terranes: A case study from the Transantarctic Mountains of southern Victoria Land. *Chemistry Geology*, 225, 91–120. <https://doi.org/10.1016/j.chemgeo.2005.09.001>
- Fitzgerald, P. G., & Gleadow, A. J. W. (1988). Fission-track geochronology, tectonics and structure of the Transantarctic Mountains in northern Victoria Land, Antarctica. *Chemistry Geology*, 73, 169–198. [https://doi.org/10.1016/0168-9622\(88\)90014-0](https://doi.org/10.1016/0168-9622(88)90014-0)
- Fitzgerald, P. G., & Stump, E. (1997). Cretaceous and Cenozoic episodic denudation of the Transantarctic Mountains, Antarctica: New constraints from apatite fission track thermochronology in the Scott Glacier region. *Journal of Geophysical Research*, 102, 7747–7765. <https://doi.org/10.1029/96JB03898>
- Fleming, T. H., Elliot, D. H., Foland, D. A., Jones, L. M., & Bowman, J. R. (1993). *Disturbance of Rb-Sr and K-Ar isotopic systems in the Kirkpatrick Basalts, north Victoria Land, Antarctica: Implications for middle Cretaceous tectonism* (pp. 411–424). Paper presented at Gondwana Eight: Assembly, Evolution and Dispersal, Proceedings of the 8th Gondwana Symposium, Balkema, Hobart.
- Gailbraith, R. F. (1981). On statistical models for fission track counts. *Mathematical Geology*, 13(6), 471–478. <https://doi.org/10.1007/BF01034498>
- Gleadow, A. J. W., & Fitzgerald, P. G. (1987). Uplift history and structure of the Transantarctic Mountains: New evidence from fission track dating of basement apatites in the Dry Valleys area, southern Victoria Land. *Earth and Planetary Science Letters*, 82, 1–14. [https://doi.org/10.1016/0012-821X\(87\)90102-6](https://doi.org/10.1016/0012-821X(87)90102-6)
- Golledge, N. R., Christopher, J. F., Andrew, N. M., & Kevin, M. B. (2012). Dynamics of the last glacial maximum Antarctic ice-sheet and its response to ocean forcing. *Proceedings of the National Academy of Sciences*, 109(40), 16,052–16,056. <https://doi.org/10.1073/pnas.1205385109>
- Goodge, J. W. (2020). Geological and tectonic evolution of the Transantarctic Mountains, from ancient craton to recent enigma. *Gondwana Research*, 80, 50–122. <https://doi.org/10.1016/j.gr.2019.11.001>
- Gunn, B. M., & Warren, G. (1962). Geology of Victoria Land between the Mawson and Mulock Glaciers, Antarctica. *New Zealand Journal of Geology and Geophysics*, 5(3), 407–426. <https://doi.org/10.1080/00288306.1962.10420097>
- Hauptvogel, D. W., & Passchier, S. (2012). Early–Middle Miocene (17–14 Ma) Antarctic ice dynamics reconstructed from the heavy mineral provenance in the AND-2A drill core, Ross Sea, Antarctica. *Global and Planetary Change*, 82–83, 38–50. <https://doi.org/10.1016/j.gloplacha.2011.11.003>
- Huerta, A., Blythe, A. E., & Utevsky, E. (2011). *Collapse of a Mesozoic West Antarctic plateau: Evidence from low temperature thermochronology and geodynamical modelling*. Paper presented at Geological Society American Annual Meeting, Minneapolis, USA.
- Hughes, T. J. (1977). West Antarctic ice streams. *Reviews of Geophysics and Space Physics*, 15(1), 1–46. <https://doi.org/10.1029/RG015i001p00001>
- Hurford, A. J. (1990). International Union of Geological Sciences Subcommission on Geochronology recommendation for the standardization of fission track dating calibration and data reporting. *Nuclear Tracks*, 17, 233–236. [https://doi.org/10.1016/1359-0189\(90\)90040-5](https://doi.org/10.1016/1359-0189(90)90040-5)
- Hurford, A. J., & Green, P. F. (1983). The zeta age calibration of fission track dating. *Chemistry Geology*, 1, 285–317. [https://doi.org/10.1016/S0009-2541\(83\)80026-6](https://doi.org/10.1016/S0009-2541(83)80026-6)
- Kellogg, T. B., Truesdale, R. S., & Osterman, L. E. (1979). Late Quaternary extent of the West Antarctic Ice Sheet: New evidence from the Ross Sea cores. *Geology*, 7(5), 249–253. [https://doi.org/10.1130/0091-7613\(1979\)7%3C249:LQEOOTW%3E2.0.CO;2](https://doi.org/10.1130/0091-7613(1979)7%3C249:LQEOOTW%3E2.0.CO;2)
- Ketcham, R. A. (2005). The role of crystallographic angle in characterizing and modeling apatite fission-track length data. *Radiation Measurements*, 39, 595–601. <https://doi.org/10.1016/j.radmeas.2004.07.008>
- Korhonen, F. J., Saito, S., Brown, M., Siddoway, C. S., & Day, J. M. D. (2010a). Multiple generations of granite in the Fosdick Mountains, Marie Byrd Land, West Antarctica; implications for polyphase intracrustal differentiation in a continental margin setting. *Journal of Petrology*, 51(3), 627–670. <https://doi.org/10.1093/petrology/egp093>
- Korhonen, F. J., Saito, S., Brown, M., Siddoway, C. S., & Day, J. M. D. (2010b). Modeling multiple melt loss events in the evolution of an active continental margin. *Lithos*, 116(3–4), 230–248. <https://doi.org/10.1016/j.lithos.2009.09.004>
- Kyle, P. R. (1981). Glacial history of the McMurdo Sound area, as indicated by the distribution and nature of McMurdo volcanic rocks in the Dry Valley Drilling Project. In L. D. McGinnis (Ed.), *Dry Valley Drilling Project, Antarctic Research Series* (Vol. 33, pp. 403–412). Washington, DC: American Geophysical Union. <https://doi.org/10.1029/AR033>
- Kyle, P. R. (1990). McMurdo Volcanic Group, western Ross Embayment—Introduction. In W. E. L. LeMasurier, & J. W. Thomson (Eds.), *Volcanoes of the Antarctic Plate and Southern Oceans, Antarctic Research Series* (Vol. 48, pp. 19–25). Washington, DC: American Geophysical Union. <https://doi.org/10.1029/AR048>
- LeMasurier, W. E. (2008). Neogene extension and basin deepening in the West Antarctic rift inferred from comparisons with the East African rift and other analogs. *Geology*, 36, 247–250. <https://doi.org/10.1130/G24363A.1>
- LeMasurier, W. E., Choi, S. H., Kawachi, Y., Mukasa, S. B., & Rogers, N. W. (2011). Evolution of pantellerite-trachyte-phonolite volcanoes by fractional crystallization of basanite magma in a continental rift setting, Marie Byrd Land, Antarctica. *Contributions to Mineralogy and Petrology*, 162(6), 1175–1199. <https://doi.org/10.1007/s00410-011-0646-z>
- LeMasurier, W. E., & Landis, C. A. (1996). Mantle-plume activity recorded by low-relief erosion surfaces in West Antarctica and New Zealand. *Geological Society of America Bulletin*, 108(11), 1450–1466. [https://doi.org/10.1130/0016-7606\(1996\)108%3C1450:MPARBL%3E2.3.CO;2](https://doi.org/10.1130/0016-7606(1996)108%3C1450:MPARBL%3E2.3.CO;2)
- Li, X., Zattin, M., & Olivetti, V. (2019). A detrital apatite fission-track study of the CIROS-2 sedimentary record: Tracing ice pathways in the Ross Sea area over the last 5 Ma. *Terra Nova*, 31(3), 271–280. <https://doi.org/10.1111/ter.12396>

- Licht, K. J., & Andrews, J. T. (2002). A ^{14}C record of late Pleistocene ice advance and retreat in the central Ross Sea, Antarctica. *Arctic, Antarctic, and Alpine Research*, 34(3), 324–333. <https://doi.org/10.1080/15230430.2002.12003501>
- Licht, K. J., Dunbar, N. W., Andrews, J. T., & Jennings, A. E. (1999). Distinguishing subglacial till and glacial marine diamictites in the western Ross Sea, Antarctica: Implications for a last glacial maximum grounding line. *Bulletin of the Geological Society of America*, 111(1), 91–103. [https://doi.org/10.1130/0016-7606\(1999\)111%3C0091:DSTAGM%3E2.3.CO;2](https://doi.org/10.1130/0016-7606(1999)111%3C0091:DSTAGM%3E2.3.CO;2)
- Licht, K. J., & Fastook, J. (1998). *Constraining a numerical ice sheet model with geologic data over one ice sheet advance/retreat cycle in the Ross Sea* (pp. 25–26). Paper presented at the Chapman Conference on the West Antarctic Ice Sheet, University of Maine.
- Licht, K. J., & Hemming, S. (2017). Analysis of Antarctic glaciogenic sediment provenance through geochemical and petrologic applications (Invited Review). *Quaternary Science Reviews*, 164, 1–24. <https://doi.org/10.1016/j.quascirev.2017.03.009>
- Licht, K. J., Hennessy, A. J., & Welke, B. M. (2014). The U-Pb detrital zircon signature of West Antarctic ice stream tills in the Ross Embayment, with implications for Last Glacial Maximum ice flow reconstructions. *Antarctic Science*, 26(6), 687–697. <https://doi.org/10.1017/S0954102014000315>
- Licht, K. J., Jennings, A. E., Andrews, J. T., & Williams, K. M. (1996). Chronology of late Wisconsin ice retreat from the western Ross Sea, Antarctica. *Geology*, 24(3), 223–226. [https://doi.org/10.1130/0091-7613\(1996\)024%3C0223:COLWIR%3E2.3.CO;2](https://doi.org/10.1130/0091-7613(1996)024%3C0223:COLWIR%3E2.3.CO;2)
- Licht, K. J., Lederer, J. R., & Swope, R. J. (2005). Provenance of LGM glacial till (sand fraction) across the Ross Embayment, Antarctica. *Quaternary Science Reviews*, 24, 1499–1520. <https://doi.org/10.1016/j.quascirev.2004.10.017>
- Lisker, F. (1996). Geodynamik des Westantarktischen Riftsystems basierend auf Apatit-Spaltspuranalysen. *Reports Polar Research*, 198, 1–108. https://doi.org/10.2312/bzp_0198_1996
- Lisker, F. (2002). Review of fission track studies in northern Victoria Land, Antarctica—Passive margin evolution versus uplift of the Transantarctic Mountains. *Tectonophysics*, 349, 57–73. [https://doi.org/10.1016/S0040-1951\(02\)00046-X](https://doi.org/10.1016/S0040-1951(02)00046-X)
- Lisker, F., & Laufer, A. (2013). The Mesozoic Victoria Basin: Vanished link between Antarctica and Australia. *Geology*, 41, 1043–1046. <https://doi.org/10.1130/G33409.1>
- Lisker, F., Läufer, A., Olesch, M., Rossetti, F., & Schäfer, T. (2006). The Transantarctic Beacon Basin: New insights from AFT data and structural data from the USARP Mountains and adjacent areas (northern Victoria Land, Antarctica). *Basin Research*, 18, 497–520. <https://doi.org/10.1111/j.1365-2117.2006.00301.x>
- Lisker, F., & Olesch, M. (1998). Cooling and denudation history of western Marie Byrd Land, Antarctica, based on apatite fission-tracks. https://doi.org/10.1007/978-94-015-9133-1_14
- Luyendyk, B. P., Wilson, D. S., & Siddoway, C. S. (2003). Eastern margin of the Ross Sea Rift in western Marie Byrd Land, Antarctica: Crustal structure and tectonic development. *Geochemistry, Geophysics, Geosystems*, 4(10), 1090. <https://doi.org/10.1029/2002GC000462>
- Malusà, M. G., & Garzanti, E. (2019). The sedimentology of detrital thermochronology. In M. G. Malusà, & P. G. Fitzgerald (Eds.), *Fission-Track Thermochronology and Its Application to Geology* (pp. 123–143). Cham: Springer. <https://doi.org/10.1007/978-3-319-89421-8>
- Marchant, D. R., Swisher, C. C., & Berkeley, I. (1996). Late Cenozoic Antarctic paleoclimate reconstructed from volcanic ashes in the Dry Valleys region of southern Victoria Land. *Bulletin of the Geological Society of America*, 2, 181–194. [https://doi.org/10.1130/0016-7606\(1996\)018%3C0181:LCAPRF%3E2.3.CO;2](https://doi.org/10.1130/0016-7606(1996)018%3C0181:LCAPRF%3E2.3.CO;2)
- McKay, R. M., Dunbar, G. B., Naish, T. R., Barrett, P. J., Carter, L., & Harper, M. (2008). Retreat history of the Ross Ice Sheet (Shelf) since the Last Glacial Maximum from deep-basin sediment cores around Ross Island. *Palaeogeography, Palaeoclimatology, Palaeoecology*, 260(1–2), 245–261. <https://doi.org/10.1016/j.palaeo.2007.08.015>
- Miller, S. R., Fitzgerald, P. G., & Baldwin, S. L. (2010). Cenozoic range front faulting and development of the Transantarctic Mountains near Cape Surprise, Antarctica: Thermochronologic and geomorphologic constraints. *Tectonics*, 29, TC1003. <https://doi.org/10.1029/2009TC002457>
- Molzahn, M., Wörner, G., Henjes-Kunst, F., & Rocholl, A. (1999). Constraints on the Cretaceous thermal event in the Transantarctic Mountains from alteration processes in Ferrar flood basalts. *Global and Planetary Change*, 23, 45–60. [https://doi.org/10.1016/S0921-8181\(99\)00050-8](https://doi.org/10.1016/S0921-8181(99)00050-8)
- Mosola, A. B., & Anderson, J. B. (2006). Expansion and rapid retreat of the West Antarctic Ice Sheet in eastern Ross Sea: Possible consequence of over-extended ice streams? *Quaternary Science Reviews*, 25, 2177–2196. <https://doi.org/10.1016/j.quascirev.2005.12.013>
- Mukasa, S. B., & Dalziel, I. W. D. (2000). Marie Byrd Land, West Antarctica: Evolution of Gondwana's Pacific margin constrained by zircon U-Pb geochronology and feldspar common-Pb isotopic compositions. *Bulletin of the Geological Society of America*, 112(4), 611–627. [https://doi.org/10.1130/0016-7606\(2000\)112%3C611:MBLWAE%3E2.0.CO;2](https://doi.org/10.1130/0016-7606(2000)112%3C611:MBLWAE%3E2.0.CO;2)
- Müller, P., Schmidt-Thomé, M., Kreuzer, H., Tessensohn, F., & Vetter, U. (1991). Cenozoic peralkaline magmatism at the western margin of the Ross Sea, Antarctica. *Memorie della Società Geologica Italiana*, 46, 315–336.
- Olivetti, V., Balestrieri, M. L., Rossetti, F., & Talarico, F. M. (2013). Tectonic and climatic signals from apatite detrital fission track analysis of the Cape Robert Project core records, south Victoria Land, Antarctica. *Tectonophysics*, 594, 80–90. <https://doi.org/10.1016/j.tecto.2013.03.017>
- Olivetti, V., Balestrieri, M. L., Rossetti, F., Thomson, S. N., Talarico, F. M., & Zattin, M. (2015). Evidence of a full West Antarctic Ice Sheet back to the early Oligocene: Insight from double dating of detrital apatites in Ross Sea sediments. *Terra Nova*, 27, 238–246. <https://doi.org/10.1111/ter.12153>
- Olivetti, V., Rossetti, F., Balestrieri, M. L., Pace, D., Cormamusini, G., & Talarico, F. (2018). Variability in uplift, exhumation and crustal deformation along the Transantarctic Mountains front in southern Victoria Land, Antarctica. *Tectonophysics*, 745, 229–244. <https://doi.org/10.1016/j.tecto.2018.08.017>
- Pankhurst, R. J., Weaver, S. D., Bradshaw, J. D., Storey, B. C., & Ireland, T. R. (1998). Geochronology and geochemistry of pre-Jurassic superterranes in Marie Byrd Land, Antarctica. *Journal of Geophysical Research*, 103(B2), 2529–2547. <https://doi.org/10.1029/97JB02605>
- Paxman, G. J. G., Jamieson, S. S. R., Hochmuth, K., Gohl, K., Bentley, M. J., Leitchenkov, G., & Ferraccioli, F. (2019). Reconstructions of Antarctic topography since the Eocene-Oligocene boundary. *Palaeogeography, Palaeoclimatology, Palaeoecology*, 535, 109346. <https://doi.org/10.1016/j.palaeo.2019.109346>
- Perotti, M., Andreucci, B., Talarico, F., & Zattin, M. (2017). Multi-analytical provenance analysis of Eastern Ross Sea LGM till sediments (Antarctica): Petrography, geochronology, and thermochronology detrital data. *Geochemistry, Geophysics, Geosystems*, 18, 2275–2304. <https://doi.org/10.1002/2016GC006728>
- Perotti, M., Zurli, L., Sandroni, S., Cormamusini, G., & Talarico, F. (2018). Provenance of Ross Sea Drift in McMurdo Sound (Antarctica) and implications for Middle-Quaternary to LGM glacial transport: New evidence from petrographic data. *Sedimentary Geology*, 371, 41–54. <https://doi.org/10.1016/j.sedgeo.2018.04.009>
- Pollard, D., & Deconto, R. M. (2009). Modelling West Antarctic ice sheet growth and collapse through the past five million years. *Nature*, 458(7236), 329. <https://doi.org/10.1038/nature07809>

- Pollard, D., & DeConto, R. M. (2020). Continuous simulations over the last 40 million years with a coupled Antarctic ice sheet-sediment model. *Palaeogeography, Palaeoclimatology, Palaeoecology*, 537, 109374. <https://doi.org/10.1016/j.palaeo.2019.109374>
- Prenzel, J., Lisker, F., Balestrieri, M. L., Läufer, A., & Spiegel, C. (2013). The Eisenhower Range, Transantarctic Mountains: Evaluation of qualitative interpretation concepts of thermochronological data. *Chemical Geology*, 352, 176–187. <https://doi.org/10.1016/j.chemgeo.2013.06.005>
- Prenzel, J., Lisker, F., Elsner, M., Schoner, R., Balestrieri, M. L., Läufer, A. L., et al. (2014). Burial and exhumation of the Eisenhower Range, Transantarctic Mountains, based on thermochronological, sedimentary rock maturity and petrographic constraints. *Tectonophysics*, 630, 113–130. <https://doi.org/10.1016/j.tecto.2014.05.020>
- Prenzel, J., Lisker, F., Monsees, N., Balestrieri, M. L., Läufer, A., & Spiegel, C. (2018). Development and inversion of the Mesozoic Victoria Basin in the Terra Nova Bay (Transantarctic Mountains) derived from thermochronological data. *Gondwana Research*, 53, 110–128. <https://doi.org/10.1016/j.gr.2017.04.025>
- Reiners, P. W., & Brandon, M. T. (2006). Using thermochronology to understand orogenic erosion. *Annual Review of Earth and Planetary Sciences*, 34(1), 419–466. <https://doi.org/10.1146/annurev.earth.34.031405.125202>
- Rignot, E., Bamber, J. L., Van Den Broeke, M. R., Davis, C., Li, Y., Van De Berg, W. J., & Van Meijgaard, E. (2008). Recent Antarctic ice mass loss from radar interferometry and regional climate modelling. *Nature Geoscience*, 1, 106–110. <https://doi.org/10.1038/ngeo102>
- Rocchi, S., Armienti, P., D'Orazio, M., Tonarini, S., Wijbrans, J. R., & Di Vincenzo, G. (2002). Cenozoic magmatism in the western Ross Embayment: Role of mantle plume versus plate dynamics in the development of West Antarctic Rift System. *Journal of Geophysical Research*, 107(B9), 2195. <https://doi.org/10.1029/2001JB000515>
- Saito, S., Brown, M., Korhonen, F. J., McFadden, R. R., & Siddoway, C. S. (2013). Petrogenesis of Cretaceous mafic intrusive rocks, Fosdick Mountains, West Antarctica: Melting of the sub-continental arc mantle along the Gondwana margin. *Gondwana Research*, 23(4), 1567–1580. <https://doi.org/10.1016/j.gr.2012.08.002>
- Sandroni, S., & Talarico, F. M. (2006). Analysis of clast lithologies from CIROS-2 core, New Harbour, Antarctica—Implications for ice flow directions during Plio-Pleistocene time. *Palaeogeography, Palaeoclimatology, Palaeoecology*, 231, 215–232. <https://doi.org/10.1016/j.palaeo.2005.07.031>
- Shipp, S., Anderson, J. B., & Domack, E. W. (1999). Late Pleistocene-Holocene retreat of the West Antarctic Ice Sheet system in the Ross Sea: Part 1—Geophysical results. *Bulletin of the Geological Society of America, London, Special Publications*, 203(1), 277–304. [https://doi.org/10.1130/0016-7606\(1999\)111%3C1486:LPHROT%3E2.3.CO;2](https://doi.org/10.1130/0016-7606(1999)111%3C1486:LPHROT%3E2.3.CO;2)
- Shipp, S. S., Wellner, J. S., & Anderson, J. B. (2002). Retreat signature of a polar ice stream: Sub-glacial geomorphic features and sediments from the Ross Sea, Antarctica. *Bulletin of the Geological Society of America, London, Special Publications*, 203(1), 277–304. <https://doi.org/10.1144/GSL.SP.2002.203.01.15>
- Siddoway, C. S., Baldwin, S. L., Fitzgerald, P. G., Fanning, C. M., & Luyendyk, B. P. (2004). Ross Sea mylonites and the timing of intra-continental extension within the West Antarctic rift system. *Geology*, 32(1), 57–60. <https://doi.org/10.1130/G20005.1>
- Siddoway, C. S., Richard, S. M., Fanning, C. M., & Luyendyk, B. P. (2004). Origin and emplacement of a Middle Cretaceous gneiss dome, Fosdick Mountains, West Antarctica. In D. L. Whitney, C. Teyssier, & C. S. Siddoway (Eds.), *Gneiss domes in Orogeny, Special Paper* (Vol. 380, pp. 267–294). Boulder, CO: The Geological Society of America. <https://doi.org/10.1130/0-8137-2380-9.267>
- Siddoway, C. S., Sass, L. C., & Esser, R. P. (2005). Kinematic history of the Marie Byrd Land terrane, West Antarctica: Direct evidence from Cretaceous mafic dykes. In A. Vaughan, P. Leat, & R. J. Pankhurst (Eds.), *Terrane Processes at the Margin of Gondwana, Special Publications* (Vol. 246, pp. 417–438). London: Geological Society. <https://doi.org/10.1144/GSL.SP.2005.246.01.17>
- Spiegel, C., Lindow, J., Kamp, P. J. J., Meisel, O., Mukasa, S., Lisker, F., et al. (2016). Tectonomorphic evolution of Marie Byrd Land—Implications for Cenozoic rifting activity and onset of West Antarctic glaciation. *Global and Planetary Change*, 145, 98–115. <https://doi.org/10.1016/j.gloplacha.2016.08.013>
- Storti, F., Balestrieri, M. L., Balsamo, F., & Rossetti, F. (2008). Structural and thermochronological constraints on the evolution of the West Antarctic Rift System in central Victoria Land. *Tectonics*, 27, TC4012. <https://doi.org/10.1029/2006TC002066>
- Stuiver, M., Denton, G. H., Hughes, T. J., & Fastook, J. L. (1981). History of the marine ice sheets in West Antarctica during the last glaciation: A working hypothesis. In G. H. Denton, & T. Hughes (Eds.), *The Last Great Ice Sheets* (pp. 319–439). New York: Wiley-Interscience.
- Stump, E., & Fitzgerald, P. G. (1992). Episodic uplift of the Transantarctic Mountains. *Geology*, 20, 161–164. [https://doi.org/10.1130/0091-7613\(1992\)020%26lt;0161:EUOTTM%26gt;2.3.CO;2](https://doi.org/10.1130/0091-7613(1992)020%26lt;0161:EUOTTM%26gt;2.3.CO;2)
- Tinto, K. J., Padman, L., Siddoway, C. S., Springer, S. R., Fricker, H. A., Das, I., et al. (2019). Ross Ice Shelf response to climate driven by the tectonic imprint on seafloor bathymetry. *Natural Geoscience*, 12(6), 441–449. <https://doi.org/10.1038/s41561-019-0370-2>
- Vermesch, P. (2013). Multi-sample comparison of detrital age distributions. *Chemical Geology*, 341, 140. <https://doi.org/10.1016/j.chemgeo.2013.01.010>
- Weaver, S. D., Adams, C. J., Pankhurst, R., %26 Gibson, I. L. (1992). Granites of Edward VII Peninsula, Marie Byrd Land: Anorogenic magmatism related to Antarctic-New Zealand rifting. *Earth and Environmental Science Transactions of the Royal Society of Edinburgh*, 83(1–2), 281–290. <https://doi.org/10.1017/S0263593300007963>
- Weaver, S. D., Bradshaw, J. D., %26 Adams, C. J. (1991). Granitoids of the Ford Ranges, Marie Byrd Land, Antarctica. In M. R. A. Thompson (Ed.), *Geological Evolution of Antarctica* (pp. 345–351). Cambridge: Cambridge University Press.
- Welke, B., Licht, K., Hennessy, A., Hemming, S., Pierce Davis, E., %26 Kassab, C. (2016). Applications of detrital geochronology and thermochronology from glacial deposits to the Paleozoic and Mesozoic thermal history of the Ross Embayment, Antarctica. *Geochemistry, Geophysics, Geosystems*, 17, 2762–2780. <https://doi.org/10.1002/2015GC005941>
- Zattin, M., Andreucci, B., Thomson, S. N., Reiners, P. W., %26 Talarico, F. M. (2012). New constraints on the provenance of the ANDRILL AND-2A succession (western Ross Sea, Antarctica) from apatite triple dating. *Geochemistry, Geophysics, Geosystems*, 13, Q10016. <https://doi.org/10.1029/2012GC004357>
- Zattin, M., Pace, D., Andreucci, B., Rossetti, F., %26 Talarico, F. M. (2014). Cenozoic erosion of Transantarctic Mountains: A source-to-sink thermochronological study. *Tectonophysics*, 630, 158–165. <https://doi.org/10.1016/j.tecto.2014.05.022>
- Zattin, M., Talarico, F., %26 Sandroni, S. (2010). Integrated provenance and detrital thermochronology studies in the ANDRILL AND-2A drill core: Late Oligocene-Early Miocene exhumation of the Transantarctic Mountains (southern Victoria Land, Antarctica). *Terra Nova*, 22, 361–368. <https://doi.org/10.1111/j.1365-3121.2010.00958.x>
- Zundel, M., Spiegel, C., Lisker, F., %26 Monien, P. (2019). Post mid-Cretaceous tectonic and topographic evolution of Western Marie Byrd Land, West Antarctica: Insights from apatite fission track and (U-Th-Sm)/He data. *Geochemistry, Geophysics, Geosystems*, 20, 5831–5848. <https://doi.org/10.1029/2019GC008667>